

1972

# A nuclear quadrupole resonance study of heavy transition metal halide compounds with bridging halogen atoms

Paul Alan Edwards  
*Iowa State University*

Follow this and additional works at: <https://lib.dr.iastate.edu/rtd>

 Part of the [Inorganic Chemistry Commons](#)

## Recommended Citation

Edwards, Paul Alan, "A nuclear quadrupole resonance study of heavy transition metal halide compounds with bridging halogen atoms " (1972). *Retrospective Theses and Dissertations*. 5905.  
<https://lib.dr.iastate.edu/rtd/5905>

This Dissertation is brought to you for free and open access by the Iowa State University Capstones, Theses and Dissertations at Iowa State University Digital Repository. It has been accepted for inclusion in Retrospective Theses and Dissertations by an authorized administrator of Iowa State University Digital Repository. For more information, please contact [digirep@iastate.edu](mailto:digirep@iastate.edu).

73-3878

EDWARDS, Paul Alan, 1948-  
A NUCLEAR QUADRUPOLE RESONANCE STUDY OF HEAVY  
TRANSITION METAL HALIDE COMPOUNDS WITH  
BRIDGING HALOGEN ATOMS.

Iowa State University, Ph.D., 1972  
Chemistry, inorganic

University Microfilms, A XEROX Company, Ann Arbor, Michigan

A nuclear quadrupole resonance study of  
heavy transition metal halide  
compounds with bridging halogen atoms

by

Paul Alan Edwards

A Dissertation Submitted to the  
Graduate Faculty in Partial Fulfillment of  
The Requirements for the Degree of  
DOCTOR OF PHILOSOPHY  
Department: Chemistry  
Major: Inorganic Chemistry

Approved:

Signature was redacted for privacy.

In Charge of Major Work

Signature was redacted for privacy.

For the Major Department

Signature was redacted for privacy.

For the Graduate College

Iowa State University  
Ames, Iowa

1972

PLEASE NOTE:

Some pages may have  
indistinct print.

Filmed as received.

University Microfilms, A Xerox Education Company

## TABLE OF CONTENTS

	Page
INTRODUCTION	1
Review of Previous Work	2
Theory of Nuclear Quadrupole Resonance	12
Interpretation of Nuclear Quadrupole Resonance Data	23
EXPERIMENTAL PROCEDURES	35
Synthesis of the Metal Pentahalides	35
Nuclear Quadrupole Resonance Spectra	35
Numerical Interpretation of Data	47
ASSIGNMENT OF RESONANCES	48
Niobium Pentahalides	48
Tantalum Pentahalides	51
Related Metal Pentahalides	57
INTERPRETATION	63
Interpretation of Metal Resonances	63
Interpretation of Halogen Resonances	68
SUMMARY	74
SUGGESTIONS FOR FUTURE WORK	75
ACKNOWLEDGEMENTS	78
BIBLIOGRAPHY	80
APPENDIX	84

## INTRODUCTION

The study of heavy transition metal halide complexes using nuclear quadrupole resonance (nqr) techniques is an inviting venture for several reasons. Probably foremost is the possibility of being able to study more than one element in a compound. For example, in compounds containing niobium or tantalum and either chlorine, bromine, or iodine, the possibility of detecting metal and halogen atom resonances does exist. It goes almost without saying that the more resonance information that can be gathered about a compound, the better the bonding and then, hopefully, the chemistry of the compound can be understood. The structural aspect of many heavy transition metal halide complexes is also a consideration in two respects. First, many of these compounds contain two distinct types of halogen atoms: bridging and terminal. The ability to reliably distinguish between bridging and terminal halogen atoms to such a degree that sound predictions can be made about the structure of compounds without actually having to do a complete single crystal X-ray structural determination is an exciting prospect. Second, many of these compounds are of interest because they exist as polynuclear species ranging from the  $M_2X_{10}$  species studied in this thesis to the hexanuclear  $M_6X_{18}^{n-}$  cluster anions. Nuclear quadrupole resonance studies could provide valuable probes

into the bonding in these polynuclear species.

The research to be described in this thesis was undertaken in the hope of demonstrating the feasibility of studying heavy transition metal halide complexes using nqr techniques. In particular this thesis will address itself to the issue of reliably distinguishing between bridging and terminal halogen atoms in compounds of known structure. Additionally, the possibility of answering some of the questions alluded to in the preceding paragraph will be discussed.

Review of Previous Work.--Heavy transition metal halides have been of interest to nqr spectroscopists not only for the reasons given earlier, but also for the positive temperature coefficients associated with many of the nqr frequencies. In general, nqr signals are expected to increase in frequency with decreasing temperature, *i.e.*, the temperature coefficient ( $d\nu/dT$ ) is negative. A negative coefficient is generally explained by torsional vibrations of the molecule in the crystal which tend to average or attenuate the effective field gradient around the nucleus. As torsional vibration states become less populated as a function of a decrease in temperature, the averaging effect is lessened and the resonance frequency increases proportionally to the increase in effective field gradient. Bayer<sup>1</sup> quantitatively attempted to explain this phenomenon,

but although qualitatively correct, the validity of Bayer's equation is still open to discussion.<sup>2,3</sup>

Hamlen and Koski<sup>4</sup> detected one  $^{35}\text{Cl}$  line near 10.5 MHz in  $\text{WCl}_6$  and determined that over the range 35 to  $-196^\circ\text{C}$ , it exhibited a positive temperature coefficient. They speculated  $\pi$ -bonding could be important in the compound, but they offered no concrete explanation of their observations.

Reddoch<sup>5</sup> conducted studies of  $\text{ThCl}_4$ ,  $\text{Nb}_2\text{Cl}_{10}$ , and  $\text{Ta}_2\text{Cl}_{10}$ . He detected a  $^{35}\text{Cl}$  resonance at about 5.9 MHz in  $\text{ThCl}_4$  which displayed a positive temperature coefficient over the range from  $-75$  to  $-196^\circ\text{C}$ . Again  $\pi$ -bonding was mentioned as a factor, but only a speculative explanation of the phenomenon was offered. Signals assigned as  $^{93}\text{Nb}$ ,  $^{35}\text{Cl}$ , and  $^{37}\text{Cl}$  resonances were detected in  $\text{Nb}_2\text{Cl}_{10}$ . The Nb nucleus exhibited a very large asymmetry parameter, about 32% at  $24.5^\circ\text{C}$ , and a quadrupole coupling constant of over 78 MHz. Significantly, the detection of only one  $^{35}\text{Cl}$  resonance at 13.058 MHz at  $24.5^\circ\text{C}$ , and at 13.280 MHz at  $-196^\circ\text{C}$  is completely inconsistent with the dimeric structure of the compound<sup>6</sup> which contains two types of halogen atoms (bridging and terminal). This  $^{35}\text{Cl}$  resonance was presumed to be the bridging halogen resonance purely on the basis of qualitative arguments. Reddoch also presumed that the one  $^{35}\text{Cl}$  signal observed

in  $Ta_2Cl_{10}$  at 13.39 MHz was also a bridging halogen resonance because of its proximity to the  $^{35}Cl$  resonance in  $Nb_2Cl_{10}$ .

Safin and co-workers<sup>7</sup> obtained more reasonable results for  $Ta_2Cl_{10}$  than did Reddoch. At room temperature they observed three resonances, 13.35, 13.37, and 13.39 MHz; while at  $-196^\circ C$  they observed a doublet at 12.30 MHz (mean) and a triplet at 13.36 MHz (mean).

Ikeda, Nakamura, and Kubo<sup>8</sup> were the first to point out qualitatively the correlation between  $d\pi-p\pi$  M-X bonding and the temperature dependence of Cl nqr frequencies in hexachlorometallate (IV) compounds. They argued the  $\pi$ -bonding involves the overlap of filled halogen p orbitals with the  $d_\epsilon$  formally  $t_{2g}$  metal orbitals:  $d_{xz}$ ,  $d_{yz}$ , and  $d_{xy}$ . As the metal is varied from W to Pt, the  $d_\epsilon$  orbitals become progressively more populated with metal electrons, thus reducing the ability of halogen p electrons to migrate toward the metal atom. This "shutting off" of the ability to  $\pi$ -bond is paralleled by increasingly more negative temperature coefficients. Further, Ikeda et al. suggested the positive temperature coefficients arise from the decrease of overlap of the  $\pi$ -bonding orbitals caused by thermal vibrations. Increased thermal vibrations decrease the ability of the halogen electrons to migrate toward the metal atom, thus increasing the

field gradient around the halogen atom, resulting in a higher halogen resonance frequency as the temperature is increased.

Haas and Marram<sup>9</sup> quantitatively extended the arguments of Ikeda and co-workers.<sup>8</sup> They considered the effect of two types of vibrations, M-X stretches and X-M-X deformations, on the populations of the halogen  $p\pi$  orbitals ( $p_x$  and  $p_y$ ). They concluded it is the bending vibrations, which take the halogen  $p\pi$  orbitals out of the plane of the  $d_e$  metal orbitals breaking the  $\pi$ -bond, that lead to positive temperature coefficients. Their derived equation for the temperature dependence of nqr frequencies reasonably reflects the experimental results for  $K_2OsCl_6$ ,  $K_2IrCl_6$ , and  $K_2PtCl_6$ .

Up to this point all of the relevant systems exhibiting positive temperature coefficients have been cubic and monomeric in nature. Buslaev and co-workers<sup>10</sup> suggested the sign of the temperature coefficient could be used as a criterion for assigning resonances of dimeric systems. They studied primarily the  $^{79}Br$  and  $^{81}Br$  resonances in  $Nb_2Br_{10}$ ,  $Ta_2Br_{10}$ , and  $NbOBr_3$ . At room and liquid nitrogen temperatures they observed two distinct types of halogen resonances. Within each type there were some multiplicities of resonances, but the difference in resonance frequencies within each type was much smaller than the 20 to

40 MHz separations between types of halogen resonance frequencies. In all three cases the sets of resonances at lower frequencies exhibited positive temperature coefficients. Buslaev and co-workers argued that the resonances with the positive temperature coefficients (those at lower frequencies) should be assigned to the terminal halogen atoms because 1) the metal had vacant  $t_{2g}$  orbitals available for  $\pi$ -bonding, and 2) the terminal halogens would be more likely to  $\pi$ -bond than the bridging halogens. Because the niobium and tantalum pentabromides have basically the same structure as the pentachlorides (two octahedra sharing an edge), the authors affirmed the tentative assignment of the  $^{35}\text{Cl}$  resonances in the two pentachlorides as suggested by Reddoch.<sup>5</sup> Because the 13 MHz resonances in the two compounds do exhibit negative temperature coefficients, the authors assigned them as bridging halogen resonances. The field gradient at a terminal halogen is directly proportional to the amount of unbalanced p electron density ( $U_p$ ), where  $U_p = N_z - (N_x + N_y)/2$  ( $N$  represents the population of the valence p orbitals). If the halogen was not involved in  $\pi$ -bonding, the  $p_x$  and  $p_y$  orbitals would represent non-bonding lone pairs of electrons and  $U_p = N_z - 2$ . If, however, the  $p_x$  and  $p_y$  electrons migrate toward the metal via a  $\pi$ -bond, then  $U_p$  would be smaller than expected (see next paragraph). Buslaev and

co-workers concluded that the positive temperature coefficient associated with the lower frequency resonances identifies these resonances as terminal halogen resonances, and that these terminal halogens are donating electron density into low-lying vacant d metal orbitals via a  $\pi$ -bond.

Several group IIIB trihalide dimers have been studied using nqr, particularly by Barnes and Segel, and the structure of these compounds also involves bridging and terminal halogen atoms. In all of these compounds,  $\text{Ga}_2\text{Cl}_6$ ,  $\text{Al}_2\text{Br}_6$ ,  $\text{Ga}_2\text{Br}_6$ ,  $\text{In}_2\text{Br}_6$ ,  $\text{Al}_2\text{I}_6$ ,  $\text{Ga}_2\text{I}_6$ , and  $\text{In}_2\text{I}_6$ , two types of halogen atoms were detected by nqr, but in these compounds the lower frequency resonances were assigned to the bridging rather than to the terminal atoms.<sup>11-14</sup> If the angle between the two field gradient tensors associated with the bridging halogen-metal bonds is greater than  $90^\circ$ , the resulting net field gradient tensor is less than the field gradient tensor associated with a terminal halogen-metal bond. The components of the two "bridging" tensors parallel to the metal-metal axis cancel each other, leaving two components perpendicular to this axis which reinforce each other, but whose sum is smaller in magnitude than either of the original two bonding tensors. Thus, the resonance frequency of the bridging halogen atom was lower than that of the terminal halogen atom. A single

crystal Zeeman study of  $\text{Ga}_2\text{Cl}_6$  by Peterson and Bridenbough substantiated these arguments.<sup>15</sup> Equally important is that in  $\text{Al}_2\text{I}_6$ ,  $\text{Ga}_2\text{I}_6$ ,  $\text{In}_2\text{I}_6$ , and  $\text{Ga}_2\text{Cl}_6$  all halogen atoms assigned as bridging exhibited larger asymmetry parameters than halogen atoms assigned as terminal.<sup>14,15</sup>

T. L. Brown and co-workers have made significant contributions on the correlation of the nqr spectra of hexahalometallates to the extent of  $\pi$ -bonding in the compounds. Making use of Jørgensen optical electronegativities, Brown, McDugle, and Kent<sup>16</sup> were able to separate the  $\pi$ - and  $\sigma$ -bonding effects in a series of  $\text{MCl}_6^{n-}$  compounds. In a series of Pt(IV) to W(IV) hexachloro anions, the increased number of  $d\pi$  holes is paralleled by 1) a substantial increase of charge on the metal, 2) a decrease in total metal-halogen bond covalency, 3) an increase in the  $\pi$  contribution to the bonding, but 4) a decrease in the degree of  $\pi$ -bonding per metal  $d\pi$  orbital vacancy. Brown and co-workers additionally attempted to correlate their nqr results with observed M-Cl stretching force constants for the same compounds. They did observe an increase in the force constants with increased number of 5d electrons, but this increase does not necessarily reflect increased covalency because highly polar bonds can exhibit substantial force constants as a result of electrostatic interactions between charged atoms. However, Fenske and Radtke<sup>17</sup> did observe an

increase in the metal-chlorine overlap populations in  $MCl_4^{n-}$  species and correlated it with an increase in the frequency of the M-Cl stretching mode. The results of Fenske and Radtke,<sup>17</sup> coupled with the nqr results led the authors to postulate that the increased stretching force constant does reflect an increase in covalency. Brown and Kent<sup>18</sup> extended these results by studying the temperature dependence of  $^{35}Cl$  and  $^{81}Br$  signals in many of the same hexahalometallates. They concluded 1) the lattice contribution to the total electric field gradient is not significant in comparison to the contribution made by the covalent bonding tensor, and 2) positive temperature coefficients should be an indication of the extent of metal-halogen  $\pi$ -bonding. Additionally they take issue with the arguments of Haas and Marram<sup>9</sup> that it is the bending motions of the metal-halogen bond which give rise to the diminution of the  $\pi$ -bond. Brown and Kent<sup>18</sup> suggest that the metal atom is capable of rehybridizing its orbitals to compensate for the change in position of the halogen atom, thus keeping the  $\pi$ -bond intact. However, they do point out that because of the  $r^{-3}$  dependence of the field gradient, it could be the stretching modes are responsible for the greatest change in the effective field gradient. Because metal-halogen stretching modes are not harmonic oscillators, the equilibrium M-X distance should

increase as the temperature increases. This increased distance should have a more marked effect on the  $\pi$ -overlap populations than on the  $\sigma$ -overlap population. A decrease in the  $\pi$ -overlap population should make the halogen  $p\pi$  orbitals more like lone pairs, thus causing an increase in the magnitude of the difference  $U_p = N_\sigma - N_\pi$  which results in an increased halogen resonance frequency. One compound studied by Brown and co-workers of particular interest was  $\text{Mo}_2\text{Cl}_{10}$ .  $\text{Mo}_2\text{Cl}_{10}$  is also a dimeric compound approximating two octahedra sharing an edge<sup>19</sup> and, like  $\text{Nb}_2\text{Cl}_{10}$ , it exhibited only one  $^{35}\text{Cl}$  nqr signal at  $305^\circ\text{K}$ . This resonance also had a negative temperature coefficient associated with it.

Similarly, Armstrong and Baker<sup>20</sup> concluded that their data for the potassium salts of  $\text{PtCl}_6^{2-}$ ,  $\text{IrCl}_6^{2-}$ , and  $\text{OsCl}_6^{2-}$  cannot be explained without the inclusion of a  $\pi$ -bond attenuating mechanism. Their numerical computations were based on the Haas and Marram<sup>9</sup> bending mechanism.

O'Leary and Wheeler,<sup>21</sup> however, after study of the structure and vibrations of  $\text{K}_2\text{ReCl}_6$  as a function of temperature, concluded that positive temperature coefficients observed for that compound above  $110.9^\circ\text{K}$  are the result of rotary motions rather than  $\pi$ -bonding. They propose a "softening" of the frequency of the rotary mode from about  $25\text{ cm}^{-1}$  at  $300^\circ\text{K}$  to about  $1\text{ cm}^{-1}$  at  $112^\circ\text{K}$ . The motion

involved is specifically described as a "...longitudinal rotary mode which involves librational motion of the  $\text{MX}_6^{2-}$  octahedron as a solid body." As the temperature increases, the effective depopulation of this rotary mode leads to an increased effective field gradient.

A comparison of the experimental results, particularly those of Brown and co-workers<sup>16,18</sup> with the molecular orbital calculations of Cotton and Harris,<sup>22,23</sup> yields good, but not total agreement. Conceding the possibility of improperly inferring the relative importance of  $\sigma$ - and  $\pi$ -bonding interactions in certain compounds, the bulk of the experimental evidence available to date supports a general correlation of positive temperature coefficients with  $\pi$ -bonded systems of a cubic nature ( $\text{MX}_6^{n-}$ ).<sup>18,24</sup>

It is noteworthy that the positive temperature coefficients of halogen resonances in compounds such as  $(\text{pyH})_2\text{ZnBr}_4$ ,  $\text{NH}_4\text{CuCl}_3$ , and  $[(\text{C}_2\text{H}_5)_2\text{NH}_2]_3\text{SbBr}_6$  are not yet satisfactorily explained.<sup>25-27</sup> These compounds are not as relevant to this thesis as the hexahalometallates(IV).

Three papers concerning nqr studies of  $\text{M}_6\text{X}_{12}^{n+}$  cluster compounds are germane because of their structural interest. Mackay and Schneider<sup>28</sup> searched from 2 to 16 MHz for  $^{93}\text{Nb}$  and  $^{35}\text{Cl}$  resonances in the tetraethylammonium salts of the three cluster anions  $(\text{Nb}_6\text{Cl}_{12})\text{Cl}_6^{n-}$  ( $n = 2, 3, 4$ ) with no apparent success.  $\alpha\text{-Pd}_6\text{Cl}_{12}$ ,  $\beta\text{-Pd}_6\text{Cl}_{12}$ , and

$\beta$ -Pt<sub>6</sub>Cl<sub>12</sub>, which are known to exist as the hexanuclear cluster species, were studied using nqr by van Bronswyk and Nyholm.<sup>29</sup> Because these hexanuclear clusters have no terminal halogen atoms, the assignment and interpretation of the observed <sup>35</sup>Cl resonances are relatively unambiguous. The  $\alpha$ -Pd<sub>6</sub>Cl<sub>12</sub> exhibits only one nqr signal because all of the chlorine atoms are equivalent, and the  $\beta$ -Pt<sub>6</sub>Cl<sub>12</sub> exhibits two resonances because there are two types of halogen atoms in the distorted structure. It is inferred that the  $\beta$ -Pd<sub>6</sub>Cl<sub>12</sub> exists in an undistorted structure because only one <sup>35</sup>Cl is detected. Edwards, McCarley, and Torgeson<sup>30</sup> did detect <sup>93</sup>Nb and bridging <sup>35</sup>Cl resonances in [(CH<sub>3</sub>)<sub>4</sub>N]<sub>2</sub>[(Nb<sub>6</sub>Cl<sub>12</sub>)Cl<sub>6</sub>]. The fact that only one set of Nb resonances was detected reflects the octahedral nature of the Nb<sub>6</sub>Cl<sub>12</sub><sup>2+</sup> cluster anion. The results also provided insight into the distribution of electrons in the cluster anion, and the large field gradient exhibited by the Nb atoms could be a reflection of the effect of metal-metal bonding on the field gradient of a metal atom.

Theory of Nuclear Quadrupole Resonance.--A detailed derivation of the Hamiltonian, energy levels, selection rules, and transition probabilities operative in nqr spectroscopy would be far beyond the scope of this thesis. However, before experimental results can be properly interpreted, it is necessary to understand certain physical

concepts associated with this technique. With this in mind, a brief discussion will be presented with the intention of describing the salient features of nqr theory of primary interest to inorganic chemists. The presentation given is a blend of the theoretical discussions given by Das and Hahn,<sup>2</sup> Reddoch,<sup>5</sup> and Lucken.<sup>31</sup>

In general terms nqr is the result of the interaction of the electric quadrupole moment (eQ) of a nucleus with the electric field gradient (eq) set up by the distribution of electrons around that nucleus. Specifically the Hamiltonian of interest is the sum of all possible interactions between internal nuclear charges,  $e_i$ , and external electron charges,  $e_j$ .<sup>5</sup>

$$\hat{H} = \sum_{i,j} \frac{e_i e_j}{r_{ij}} \quad (1)$$

A classical picture would begin with the calculation of the electrostatic potential energy of a nucleus with finite dimensions in the field of its surrounding electrons<sup>31</sup>

$$W_E = \int_{\tau_e} \int_{\tau_n} \frac{\rho_e(\underline{r}_e) \rho_n(\underline{r}_n)}{|\underline{r}_e - \underline{r}_n|} d\tau_e d\tau_n \quad (2)$$

where, respectively,  $\rho_e$  and  $\rho_n$  are the electron charge density and the nuclear charge density;  $d\tau_e$  and  $d\tau_n$  are the

electron and nuclear volume elements; and  $\underline{r}_e$  and  $\underline{r}_n$  are the vectors from the center of nuclear mass to the electron and nuclear volume elements. Normalized spherical harmonics,  $Y_\ell^m(\theta, \phi)$ , are used to expand the denominator of the integral as

$$\frac{1}{|\underline{r}_e - \underline{r}_n|} = 4\pi \sum_{\ell=0}^{\infty} \sum_{m=-\ell}^{\ell} \frac{1}{2\ell + 1} \frac{r_{<}^\ell}{r_{>}^{\ell+1}} Y_\ell^{+m}(\theta_e, \phi_e) Y_\ell^{-m}(\theta_n, \phi_n) \quad (3)$$

where  $r_{<}$  and  $r_{>}$  represent the smaller and the larger of the two radius vectors, respectively. The cases in which  $\underline{r}_e < \underline{r}_n$  can be neglected because only s electrons have appreciable density inside the nucleus, and because of the spherical nature of the s orbital they cannot contribute to the field gradient. Complete separation of electronic and nuclear coordinates leads to

$$W_E = \sum_{\ell} \sum_m N_\ell^m \cdot E_\ell^{-m} \quad (4)$$

where

$$N_\ell^m = \sqrt{\frac{4\pi}{2\ell + 1}} \int \rho_n(\underline{r}_n) r_n^\ell Y_\ell^m(\theta_n, \phi_n) d\tau_n \quad (5)$$

$$E_\ell^{-m} = \sqrt{\frac{4\pi}{2\ell + 1}} \int \rho_e(\underline{r}_e) r_e^{-(\ell+1)} Y_\ell^{-m}(\theta_e, \phi_e) d\tau_e \quad (6)$$

In turn these two quantities  $E_\ell^{-m}$  and  $N_\ell^m$  can be thought of as expectation values of Hamiltonians  $\hat{E}_\ell^{-m}$  and  $\hat{N}_\ell^m$  over electronic and nuclear wavefunctions, respectively. If a nucleus of mass number  $A$  can be described by a wavefunction  $\psi(R_1 R_2 \dots R_A)$  of the coordinates of its  $A$  nucleons, then

$$\hat{N}_\ell^m = \sqrt{\frac{4\pi}{2\ell + 1}} \sum_j e_j R_j^\ell Y_\ell^m(\Theta_j, \Phi_j) \quad (7)$$

where  $e_j$  is the nucleonic charge ( $e$  for a proton and zero for a neutron), and similarly

$$\hat{E}_\ell^{-m} = e \sqrt{\frac{4\pi}{2\ell + 1}} \sum_k r_k^{-(\ell+1)} Y_\ell^{-m}(\Theta_k, \Phi_k) \quad (8)$$

Nuclear coordinates are now denoted in capital symbols and electronic coordinates, in lower case symbols. Thus the Hamiltonian for the electrostatic interaction can be written

$$\hat{H}_E = \sum_m \sum_\ell \hat{N}_\ell^m \cdot \hat{E}_\ell^{-m} \quad (9)$$

The specific Hamiltonian operative in nqr can be arrived at by examining each term of the sum as a function of  $\ell$ . Only terms with even values of  $\ell$  lead to observable

multipole moments because  $\hat{N}_\ell^m$  is the integral of an even or odd function as  $Y_\ell^m(\Theta, \Phi)$  is an even or odd function since  $R_j^\ell$  is even in all cases. But,  $Y_\ell^m(\Theta, \Phi)$  is even or odd as  $\ell$  is even or odd and integrals of odd functions are zero. The case of  $\ell = 0$  is a simple point charge interaction, so only even  $\ell$  terms with  $\ell \geq 2$  are of interest. In comparison to terms with  $\ell = 2$ , terms of  $\ell \geq 4$  can be shown to be very small, so the Hamiltonian of specific interest is<sup>2</sup>

$$\hat{H}_Q = \underline{Q} \cdot \underline{\nabla E} = \sum_m Q_2^m (\underline{\nabla E})_2^{-m} \quad (10)$$

where  $\underline{Q}$  is the tensor defining the quadrupole charge distribution in the nucleus, and  $\underline{\nabla E}$  is a tensor used to define the electric field gradient at the nucleus. The tensor  $\underline{Q}$  is a function of the scalar quadrupole moment  $eQ$  defined as

$$eQ = \int \rho_n \underline{r}_n^2 (3 \cos^2 \theta_{nI} - 1) d\tau_n \quad (11)$$

where  $\theta_{nI}$  is the angle which the vector  $\underline{r}_n$  makes with the nuclear spin vector. This scalar quadrupole moment can be thought of as a measure of the departure of the nucleus from spherical symmetry and is equal to zero if  $I < 1$ . The tensor  $\underline{\nabla E}$  is a symmetric, traceless tensor of rank 2, i.e., it has nine components,  $V_{ij}$ . In Cartesian

coordinates  $V_{ij}$  is defined

$$V_{ij} = \frac{\partial^2 V}{\partial x_i \partial x_j} \quad (x_i, x_j = x, y, z) \quad (12)$$

where  $V$  is the electrostatic potential at the nucleus produced by nearby charges such as electrons or ions. The physical significance of  $\nabla_{\sim} E$  being a traceless tensor is the field gradient at the nucleus is produced only by charges outside of the nucleus. After a transformation of axes, the irreducible components of this tensor can be written as

$$\begin{aligned} (\nabla_{\sim} E)_0 &= \frac{1}{2} V_{ZZ} = \frac{1}{2} eq \\ (\nabla_{\sim} E)_{\pm 1} &= 0 \\ (\nabla_{\sim} E)_{\pm 2} &= \frac{1}{2\sqrt{6}} (V_{XX} - V_{YY}) = \frac{1}{2\sqrt{6}} \eta eq \end{aligned} \quad (13)$$

As a result of this transformation of axes, all off-diagonal elements of the tensor  $V_{ij} (i \neq j)$  become zero and the three remaining components satisfy Laplace's equation  $V_{XX} + V_{YY} + V_{ZZ} = 0$ . Two useful definitions are made at this point. First, the quantity  $eq$ , the field gradient, is defined as  $V_{ZZ}$ ; and second, the quantity  $\eta$ , the asymmetry parameter, is defined as  $(V_{XX} - V_{YY})/V_{ZZ}$ .  $\eta$  is a measure of the departure of the field gradient from axial symmetry and with the convention

$|V_{XX}| \leq |V_{YY}| \leq |V_{ZZ}|$  can vary from 0 to 1 with,  $\eta = 0$  representing an axially symmetric field gradient.

The energies associated with this Hamiltonian can be found by evaluating, in the case of an axially symmetric field gradient, matrix elements of the type

$$(\hat{H}_Q)_{m,m} = E_m = \langle m | \hat{H}_Q | m \rangle = \frac{e^2 Qq}{4I(2I-1)} [3m^2 - I(I+1)] \quad (14)$$

where  $m$  is now a magnetic quantum number ranging in value from  $-I$  to  $+I$ , where  $I$  represents the nuclear spin, in steps of  $\Delta m = 1$ . It is important to note the energies are independent of the sign of  $m$ ; hence,  $E_m = E_{-m}$ . Transitions of a characteristic frequency  $\nu_R$  are then possible between two states  $m$  and  $m'$  for a nucleus with a given  $I$  and  $eQ$ , surrounded by a given  $eq$  when

$$\nu_R = \frac{3}{4} \frac{e^2 Qq}{hI(2I-1)} (2|m_I| - 1) \quad (15)$$

where  $m_I$  is the larger of the two magnetic quantum numbers for  $\Delta m = 1$ . In cases in which the field gradient is not axially symmetric, the situation is a little more complex because the Hamiltonian is not diagonal. Now rather than simply evaluating matrix elements of the type  $(\hat{H}_Q)_{m,m}$ , there are off-diagonal elements of the type

$$(H_Q)_{m,m\pm 2} = A \frac{\eta}{2} [I(I+1) - m(m\pm 1)]^{\frac{1}{2}} \\ [I(I+1) - (m\pm 1)(m\pm 2)]^{\frac{1}{2}} \quad (16)$$

which must be included. The Hamiltonian must be diagonalized resulting in the formation of secular equations (see Table I) characteristic of specific nuclear spins which can only be precisely solved for the  $I = 3/2$  case. Approximate solutions to these secular equations are listed in Table II. However, these solutions break down, particularly for  $\nu_1$  and  $\nu_2$  transitions in large nuclear spin systems when  $\eta$  becomes larger than approximately 0.25. For cases where  $\eta > \text{ca. } 0.25$ , procedures described by Livingston and Zeldes<sup>32</sup> for the spin 5/2 case, Reddoch<sup>5</sup> for the spin 9/2 case, or Cohen<sup>33</sup> for the spin 5/2, 7/2, or 9/2 cases must be used. The equations listed in Table II represent all the transitions possible under the restriction of  $\Delta m = 1$ . As Cohen<sup>33</sup> pointed out, this selection rule breaks down. As  $\eta$  gets large ( $> \text{ca. } 30\%$ ),  $\Delta m = 2$  transitions gain in transition probability.

It should be noted for the case  $I = 3/2$ , only one transition is possible,  $\pm 1/2 \leftrightarrow \pm 3/2$ . This means the quantities of experimental interest, the quadrupole coupling constant ( $e^2 Qq/h$ ) and the asymmetry parameter ( $\eta$ ) cannot be experimentally determined solely on the

Table I  
Secular Equations for Pure Quadrupole Interaction

I	Secular Equation	Units of E
$\frac{3}{2}$ :	$E^2 - 3\eta^2 - 9 = 0$	A <sup>a</sup>
$\frac{5}{2}$ :	$E^3 - 7(3 + \eta^2)E^2 - 20(1 - \eta^2) = 0$	2A
$\frac{7}{2}$ :	$E^4 - 42\left(1 + \frac{\eta^2}{3}\right)E^2 - 64(1 - \eta^2)E + 105\left(1 + \frac{\eta^2}{3}\right)^2 = 0$	3A
$\frac{9}{2}$ :	$E^5 - 11(3 + \eta^2)E^3 - 44(1 - \eta^2)E^2 + \frac{44}{3}(3 + \eta^2)^2E + 48(3 + \eta^2)(1 - \eta^2) = 0$	6A

<sup>a</sup>A = (e<sup>2</sup>Qq)/4I(2I - 1).

Table II  
Pure Quadrupole Transition Frequencies

I	Equations
$\frac{3}{2}$ :	$\nu = \frac{1}{2} \frac{e^2 Qq}{h} \left(1 + \frac{n^2}{3}\right)^{\frac{1}{2}}$
$\frac{5}{2}$ :	$\nu_1 = \frac{3}{20} \frac{e^2 Qq}{h} (1 + 1.0926n^2 - 0.634n^4)$ $\nu_2 = \frac{6}{20} \frac{e^2 Qq}{h} (1 - 0.2037n^2 + 0.162n^4)$
$\frac{7}{2}$ :	$\nu_1 = \frac{1}{14} \frac{e^2 Qq}{h} (1 + 3.6333n^2 - 7.261n^4)$ $\nu_2 = \frac{2}{14} \frac{e^2 Qq}{h} (1 - 0.5667n^2 + 1.8595n^4)$ $\nu_3 = \frac{3}{14} \frac{e^2 Qq}{h} (1 - 0.1000n^2 - 0.0180n^4)$
$\frac{9}{2}$ :	$\nu_1 = \frac{1}{24} \frac{e^2 Qq}{h} (1 + 9.0333n^2 - 45.691n^4)$ $\nu_2 = \frac{2}{24} \frac{e^2 Qq}{h} (1 - 1.3381n^2 + 11.724n^4)$ $\nu_3 = \frac{3}{24} \frac{e^2 Qq}{h} (1 - 0.1857n^2 - 0.1233n^4)$ $\nu_4 = \frac{4}{24} \frac{e^2 Qq}{h} (1 - 0.0809n^2 - 0.0043n^4)$

basis of pure nqr spectra. This is particularly unfortunate because four of the most frequently studied nuclei  $^{35}\text{Cl}$ ,  $^{37}\text{Cl}$ ,  $^{79}\text{Br}$ , and  $^{81}\text{Br}$  have nuclear spin of  $3/2$ . It is possible theoretically and experimentally to split the degeneracy of the  $m$  and  $-m$  states, permitting the experimental determination of both  $e^2Qq/h$  and  $\eta$ , by applying a static magnetic field to the sample resulting in a Zeeman splitting of the quadrupole spectrum. This experiment is usually carried out on a single crystal sample, but it is claimed that polycrystalline samples may also be used.<sup>34,35</sup> Refer to reference 2 for a more complete discussion of the technique.

The intensity of a pure quadrupole transition is dependent on the orientation of the principal axis of the field gradient tensor with respect to the oscillating magnetic field generated at the sample coil by the radio frequency oscillator. The intensity is maximum when the principal axis is parallel to this magnetic field, and zero when the axis is perpendicular to the field. Clearly, the intensity of a signal in a polycrystalline sample is an average intensity; but this intensity factor plays a significant role in single crystal Zeeman studies.

The inference of structural information from nqr data is sometimes complicated by the observation of multiple resonances when fewer resonances are expected on the

basis of chemical evidence. This technique has proven very sensitive to crystal effects which can bring about splittings of up to 10% of the frequencies for resonances of nuclei which would have otherwise been expected to have identical resonance frequencies.<sup>36</sup> Other phenomena such as direct dipole-dipole coupling can in extreme cases lead to splitting of a line, but generally they merely broaden a line.<sup>37</sup> These subtle linewidth effects cannot generally be detected using superregenerative oscillator-detector spectrometers (see Experimental Procedures) because these spectrometers tend to destroy the "natural" shape of a line.

The opposite yet equally frustrating situation also can occur in which fewer lines than expected are detected. Defects or stresses in a crystal can cause a random variation in the field gradient (eq) and can broaden a line to such an extent it can no longer be detected. For example, these defects or stresses can be the result of impurity molecules in the lattice and mechanical or heat treatment of the sample. Vibrational motions of the molecule can also adversely affect the intensity of a resonance, hampering its detection.

#### Interpretation of Nuclear Quadrupole Resonance

Data.--In order for nqr spectroscopy to be of use to the inorganic chemist, it must be possible to infer from the

experimentally determined quadrupole coupling constant ( $e^2Qq/h$ ) and, occasionally, asymmetry parameter ( $\eta$ ) useful chemical information. Generally, this chemical information takes the form of bonding parameters such as degree of hybridization, ionic character, and orbital populations. Specifically, since the quadrupole moment ( $eQ$ ) is a constant and can generally be looked up in an appropriate reference, a potential bonding model is judged "most reasonable" or "most likely" when reasonable bonding parameters characteristic of that model can be used to calculate values which can be compared with the experimentally determined coupling constant and asymmetry parameter.

Because exact calculations of field gradients, although possible, are time consuming and presently only feasible for small molecules,<sup>31</sup> approximate methods of analysis are predominantly used. The approximate methods most widely used by nqr spectroscopists today stem from arguments first presented by Townes and Dailey.<sup>38</sup> They proposed that the experimentally determined molecular coupling constant ( $e^2Qq_{mol}/h$ ) for atoms with  $p$  valence electrons could be related to the atomic coupling constant ( $e^2Qq_{atm}/h$ ), or more correctly called, the quadrupole coupling constant for one valence  $p$  electron with wave function oriented along the bond ( $e^2Qq_{nl0}/h$ ). It

is assumed that overlap contributions, contributions from inner core electrons, and contributions from nearby atoms, molecules, or ions to the field gradient are small. The exact form of the relation is dependent on the form of the wave function for the bonding electrons in the neighborhood of the atom under investigation. For example, in a diatomic chlorine compound in which the wave function of the Cl atom has the form  $\Psi = (1 - s - d)^{\frac{1}{2}}\psi_p + s^{\frac{1}{2}}\psi_s + d^{\frac{1}{2}}\psi_d$ , the molecular coupling constant has the form  $e^2Qq = (-1 + s - d)(1 - i)e^2Qq_{310}$ , where  $s$  and  $d$  represent the amount of  $s$  orbital and  $d$  orbital character in the hybrid orbital, and  $i$  represents the ionicity.<sup>39</sup> Because the sample equation given contains little or no readily useful chemical information, part of this section will deal with the derivation of more useful equations.

A set of equations useful for interpreting the nqr data for a bridging halogen atom, which in addition to  $\sigma$ -bonding to two identical atoms B with a B-X-B angle greater than  $90^\circ$ , also  $\pi$ -bonds with the two B atoms, will be derived to illustrate the principles involved. The philosophy behind this derivation is the same as the philosophy behind the derivations of Casabella and co-workers.<sup>40</sup> First, a coordinate system and a set of hybrid orbitals must be decided upon for the halogen atom. The  $z'$  axis is chosen perpendicular to the B-X-B plane,

the x' axis is parallel to the B-B axis, and the y' axis points from the halogen perpendicular to the B-B axis.

The hybrid orbitals are chosen as

$$\begin{aligned}
 \Psi_1 &= \psi_{p_z} \\
 \Psi_2 &= \psi_s \cot\varphi + \psi_{p_y} (1 - \cot^2\varphi)^{\frac{1}{2}} \\
 \Psi_3 &= \frac{1}{\sqrt{2}} [\psi_s (1 - \cot^2\varphi)^{\frac{1}{2}} + \psi_{p_x} - \psi_{p_y} \cot\varphi] \\
 \Psi_4 &= \frac{1}{\sqrt{2}} [\psi_s (1 - \cot^2\varphi)^{\frac{1}{2}} - \psi_{p_x} - \psi_{p_y} \cot\varphi]
 \end{aligned}
 \tag{17}$$

where  $2\varphi$  is the B-X-B angle. Next, three symmetric bonding tensors designated as  $q_{\sigma 1}$ ,  $q_{\sigma 2}$ , and  $q_{\pi}$ , each with its own symmetry axis z, are defined. These three tensors are summed as components of the total field gradient tensor in the x'y'z' coordinate system with the aid of the following equations given by Das and Hahn,<sup>2</sup> and represented as a 3 by 3 matrix.

$$\begin{aligned}
 V_{z'z'} &= \frac{q}{2} (3\cos^2\theta - 1) \\
 V_{x'x'} &= \frac{q}{2} (3\sin^2\theta \cos^2\varphi - 1) \\
 V_{y'y'} &= \frac{q}{2} (3\sin^2\theta \sin^2\varphi - 1)
 \end{aligned}
 \tag{18}$$

$$\begin{aligned}
 Vx'z' &= q \sin\theta \cos\theta \cos\phi \\
 Vy'z' &= q \sin\theta \cos\theta \sin\phi \\
 Vz'y' &= q \sin^2\theta \sin\phi \cos\phi
 \end{aligned}
 \tag{18}$$

In these equations  $q$  represents either  $q_{\sigma 1}$ ,  $q_{\sigma 2}$ , or  $q_{\pi}$ ;  $\theta$  represents the angle the tensor makes with the  $z'$  axis ( $90^\circ$  for the two  $\sigma$  tensors, and  $0^\circ$  for the  $\pi$  tensor); and  $\phi$  represents the azimuthal angle ( $\phi$  and  $\psi$  for the  $q_{\sigma 1}$  and  $q_{\sigma 2}$  tensors respectively and  $0^\circ$  for the  $q_{\pi}$  tensor). In the matrix given below, the two  $\sigma$  tensors are replaced by a single tensor  $q_{\sigma}$  since the two  $\sigma$ -bonds are assumed to be identical.

$$\begin{matrix}
 & z' & & x' & & & & y' \\
 \left( \begin{array}{cccccc}
 q_{\pi} - q_{\sigma} & & & 0 & & & & 0 \\
 0 & & & q_{\sigma}(3\cos^2\phi - 1) - \frac{q_{\pi}}{2} & & & & 0 \\
 0 & & & 0 & & & & q_{\sigma}(3\sin^2\phi - 1) - \frac{q_{\pi}}{2}
 \end{array} \right) & (19)
 \end{matrix}$$

A convenient check for errors at this point is to make sure the trace of the matrix is zero. Because the matrix is diagonal, no matrix manipulation is required. If, for example, the two  $\sigma$ -bonding tensors had not been identical, there would be off-diagonal elements, and it would be necessary to solve for the eigenvalues ( $\lambda$ ) such that  $\det |A - \lambda I| = 0$ . To obtain an equation involving the

asymmetry parameter, the diagonal elements  $Vz'z'$ ,  $Vx'x'$ , and  $Vy'y'$  are merely substituted into the equation defining the asymmetry parameter  $\eta = (V_{xx} - V_{yy})/V_{zz}$ . This substitution results in the equation

$$\eta = \frac{3q_{\sigma} \cos 2\phi}{q_{\pi} - q_{\sigma}} \quad (20)$$

At this point a little care and thought is required. A statement relating the field gradient associated with a particular bond to the population of the orbital involved with that bond is needed. A field gradient in general arises from an "unbalanced" distribution of electrons. A completely filled, or for that matter a completely empty, orbital cannot contribute to the net field gradient at a nucleus. Because the system under consideration is a halogen and in general it will exist as a partially negatively charged atom, the field gradients associated with these halogen hybrid orbitals arise from a deficiency of electrons in that orbital. The equation of interest is then  $q_i = 2 - N_i$ , where  $q_i$  is the field gradient associated with the  $i$ th orbital and  $N_i$  is the population of that orbital. Clearly, the population of any given orbital can be no greater than 2, and if it is 2, the field gradient associated with that orbital is 0. Defining the population of the  $\pi$ -bonding hybrid orbital as A,

the population of the  $\sigma$ -bonding orbitals as B, and making the appropriate substitutions into equation (20) yields

$$\eta = \frac{3(2 - B)\cos 2\theta}{(B - A)} \quad (21)$$

The equation involving the atomic and molecular coupling constants is derived with the aid of two equations<sup>4</sup>

$$N_1 = \sum_k N^k |c_1^k|^2 \quad (22)$$

and

$$e^2 Q_{\text{mol}} = e^2 Q_{\text{atm}} [N_{p_z} - \frac{1}{2}(N_{p_x} + N_{p_y})] \quad (23)$$

Equation (22) relates the population ( $N_1$ ) of the  $i$ th atomic orbital to a sum, over the  $k$  hybrid orbitals in which that atomic orbital is involved, of the product of the population ( $N_k$ ) of the  $k$ th hybrid orbital and the square of the coefficient ( $c_1^k$ ) of the  $i$ th atomic orbital in that  $k$ th hybrid orbital. Equation (23) is a well known equation relating the population ( $N_p$ ) of pure p orbitals and the atomic coupling constant to the molecular coupling of an atom with only p valence electrons. The population of the hybrid orbital  $\Psi_1$  has been defined as A because it is the orbital involved in  $\pi$ -bonding and the population of the hybrid orbital  $\Psi_2$  is 2 because it

is a filled non-bonding orbital. The population of the two  $\sigma$ -bonding hybrids  $\Psi_3$  and  $\Psi_4$  has also been fixed as B. After determining the populations of the pure unhybridized p orbitals using equation (22) and substituting into expression (23) the following equation is obtained.

$$e^2Qq_{mol} = e^2Qq_{atm} \left[ A - \frac{B}{2} - 1 - \frac{1}{2}(B - 2)\cot^2\phi \right] \quad (24)$$

It is important to note in the limiting case of no  $\pi$ -interaction, i.e., the population  $A = 2$ , the two derived equations, (21) and (24), reduce to the established relations<sup>31</sup>

$$\eta = -3\cos 2\phi \quad (25)$$

and

$$\left( \frac{e^2Qq_{mol}}{e^2Qq_{atm}} \right) \left( 1 + \frac{\eta}{3} \right) = 2 - B \quad (26)$$

As powerful as these derived equations appear to be, their range of applicability leaves a little to be desired. Equations (21) and (24) and the simpler equations (25) and (26) are capable of predicting orbital populations greater than 2 for B-X-B angles greater than approximately  $105^\circ$ . Also, at lower angles close to  $90^\circ$ , the calculated populations can actually become negative.

This "blowing-up" of the equations is probably due to violation of the convention  $|V_{xx}| \leq |V_{yy}| \leq |V_{zz}|$ . When an angle is reached such that the diagonal elements no longer obey this convention, it is necessary to relabel the axes of the field gradient tensor to reestablish the convention. For example, interchanging the y and z axes, relabeling the p orbitals in the hybrid orbitals (17) written above, and going through the procedure previously outlined yields the following equations.<sup>31</sup>

$$B - A = \frac{2\eta e^2 Q q_{mol}}{3 e^2 Q q_{atm}} \quad (27)$$

$$2 - B = \left( \frac{1}{1 - \cot^2 \phi} \right) \left( 1 - \frac{\eta}{3} \right) \left( \frac{e^2 Q q_{mol}}{e^2 Q q_{atm}} \right)$$

These equations do not "blow-up" at angles greater than  $105^\circ$ . They are not, however, useful for the system originally described because the population of the  $\pi$  orbital can, according to these equations, be less than that of the  $\sigma$  orbital, which is counter to chemical intuition. However, these equations are considered appropriate for the interpretation of the  $^{14}\text{N}$  nqr data in azabenzene.<sup>31</sup> References such as Das and Hahn,<sup>2</sup> and particularly Lucken<sup>31</sup> contain equations applicable to many bonding situations. As illustrated above, it

is possible to derive equations applicable to specific systems not already treated.

Because Townes and Dailey type interpretations are essentially valence bond treatments, these interpretations suffer from all of the deficiencies of valence bond theory. One of the most salient deficiencies vis a vis interpretation of nqr data as pointed out by Cotton and Harris is the underestimation of the contribution of orbital overlap to the effective field gradient of a quadrupolar nucleus.<sup>22</sup> Cotton and Harris have developed an LCAO-MO scheme by which calculated molecular orbitals are used to calculate the effective field gradient of a quadrupolar nucleus. This scheme contains a term  $\sum_{j < i} C_i^k C_j^k S_{ij}$  where  $C_i^k$  and  $C_j^k$  are the coefficients of the ith and jth atomic orbital in the kth molecular orbital and  $S_{ij}$  is the overlap integral of the ith and jth atomic orbitals. Clearly this scheme is no better conceptually than the LCAO-MO approximation itself, but more importantly the success of such a procedure relies heavily on the reliability of the wavefunctions used. As wavefunctions become more reliable, possibly this procedure will be used more. Other semiempirical procedures have been applied to the problem of predicting resonance frequencies in particular systems. For example, Kaplansky and Whitehead<sup>41</sup> used three different procedures,

CNDO, SAVE-CNDO, and BEEM- $\pi$  to calculate  $^{35}\text{Cl}$  resonance frequencies in  $\text{BCl}_3$  and related amine and nitrile complexes. Each procedure worked reasonably well for a few of the compounds, but no one procedure worked well for all of the compounds. Until semiempirical calculations become more generally applicable, valence bond type interpretations will continue to be widely used despite the generally recognized naivety of such interpretations. Particularly, because the compounds studied in this thesis are at the present time too complex to permit reliable semiempirical calculations, only valence bond interpretations will be presented.

Two other assumptions generally made in any interpretive procedure need to be qualitatively discussed. First, in highly ionic systems a major contribution to the field gradient at a nucleus, in addition to that produced by bonding, can be an ionic or lattice contribution. The usual approach to such an ion-lattice contribution ( $e^2Qq_{\text{ionic}}$ ) is to consider all of the atoms or ions as point charges and to calculate  $e^2Qq_{\text{ionic}}$  as a function of the position of atoms or ions in the lattice and their respective charges. Such a lattice summation is a non-trivial exercise, but for ionic compounds this contribution can be significant. Second, the inner core of electrons can also contribute to the effective field

gradient of a nucleus.<sup>31</sup> The nuclear quadrupole itself induces a distortion in the spherical electron cloud around it. Additionally the valence electrons themselves polarize the inner shell of electrons, creating another contribution to the field gradient. Such polarization is referred to as Sternheimer shielding and is particularly important in cases of closed shell ions or atoms surrounded by external field gradients.

Since the experimentally determined effective field gradient is a sum of all possible contributions, the job of the nqr spectroscopist is to deduce the primary factors contributing to this field gradient. Clearly, this is not always a trivial task, and the interpretive philosophy to be used must be carefully considered.

## EXPERIMENTAL PROCEDURES

Synthesis of the Metal Pentahalides.--With the exception of tungsten pentachloride, all metal pentahalides were synthesized by the reaction of elemental halogen with high purity metal.<sup>42</sup> Samples of several of the compounds were generously provided by past and present members of Physical and Inorganic Chemistry Group X. Tungsten pentachloride, provided by Margaret Schaefer King, was prepared by the reaction of tungsten hexachloride with tungsten hexacarbonyl.<sup>43</sup> Because of the susceptibility of all of the metal pentahalides to hydrolysis and air oxidation, all manipulation of samples was carried out using vacuum techniques or in an argon or nitrogen atmosphere dry box maintained at a dew point of less than  $-75^{\circ}\text{C}$ .

Nuclear Quadrupole Resonance Spectra.--Two different nqr spectrometers were used during this study. A block diagram of the system involving a Wilks NQR-1A super-regenerative spectrometer is shown in Figure 1. This spectrometer system at present has a useful operating range of 5 to 350 MHz. Three different oscillator-detector circuits, OS-1, OS-2, and OS-3 are required to cover this frequency range. Each oscillator has associated with it several sample coils which cover particular segments of the range of each oscillator. A fourth oscillator, OS-4, has briefly but successfully been

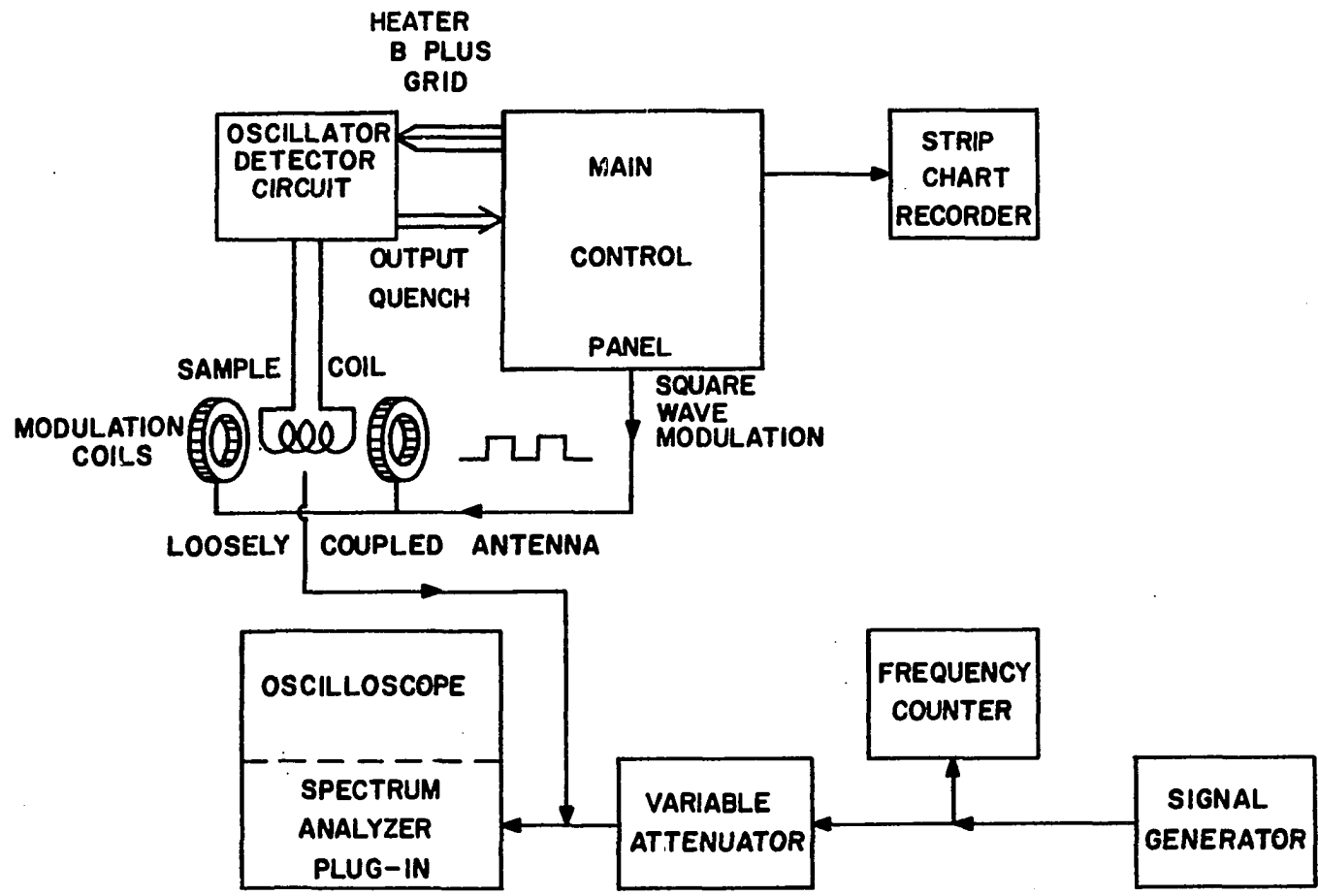


Figure 1.--Block diagram of the superregenerative spectrometer.

operated over the range 300 to 530 MHz. This oscillator is still being developed and is not yet fully operational. Das and Hahn<sup>2</sup> succinctly describe the details of the operation of a superregenerative oscillator, but several important consequences inherent in this mode of operation should be noted. Although such circuits are very sensitive, the separation of close-lying multiple resonances is extremely difficult because of the overlapping of sidebands of each resonance. Additionally, because a superregenerative oscillator-detector circuit does not respond linearly to nuclear absorption, the reliable measurement of line widths and relaxation times is virtually impossible. In the frequency range of 5 to 50 MHz a wide-line induction spectrometer<sup>30</sup> was used to obtain highly precise frequency measurements. A block diagram of that system is shown in Figure 2. This system was designed by David Torgeson of Crystal Physics Group I, and the salient features of its design and operation are given in reference 30. In this mode of operation, resonances are recorded as single derivative curves as opposed to lines complicated by sidebands. As a result, resonances as close together as 20 kHz can be easily separated.

Figure 3 provides a comparison between the salient features of the operation of the two spectrometers described above. The top half of the figure represents the

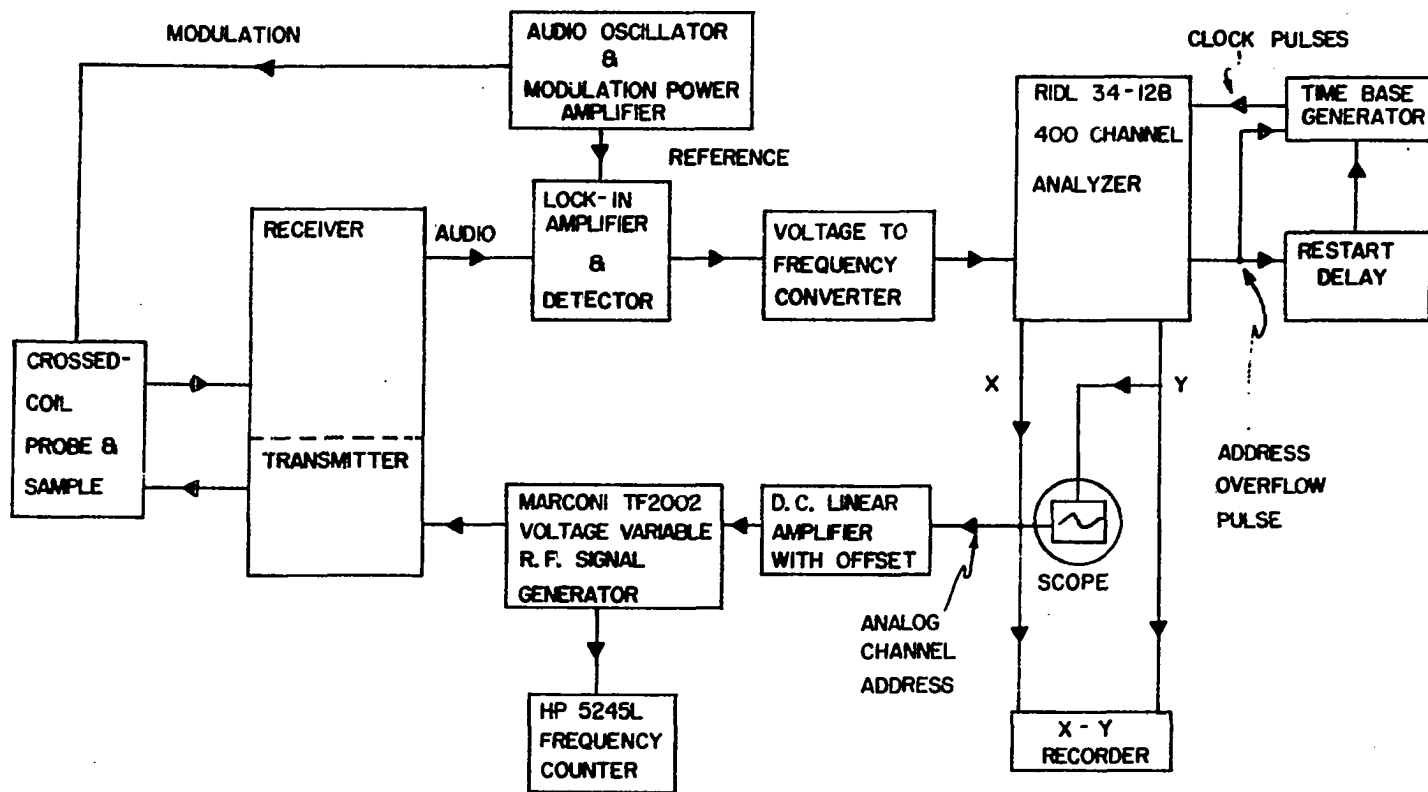
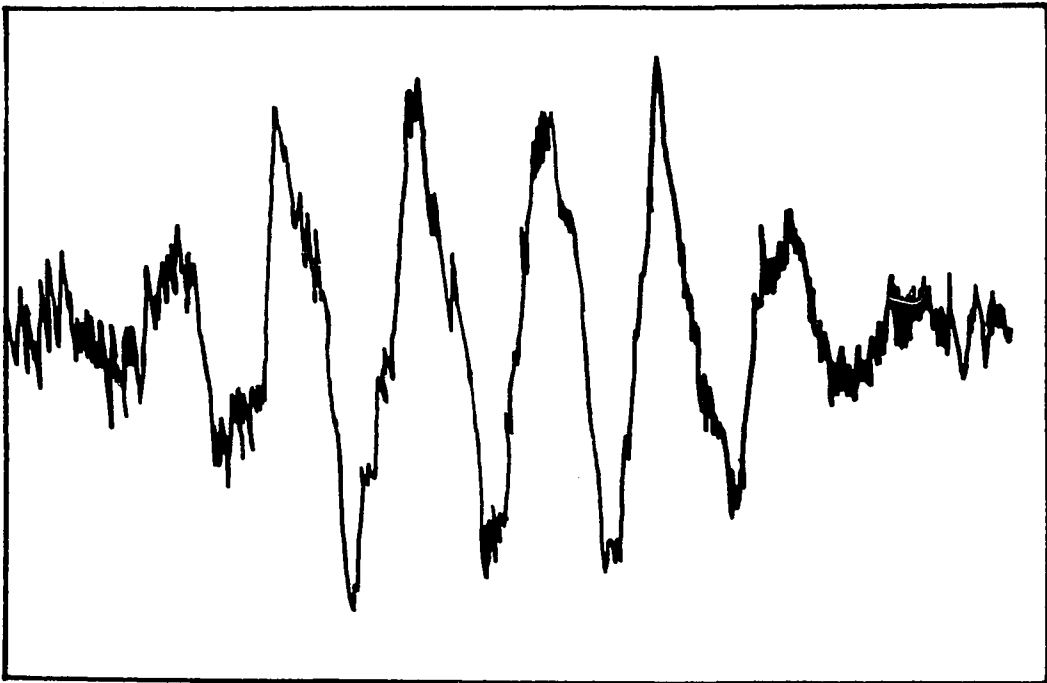


Figure 2.--Block diagram of wide-line induction spectrometer.



~ 14 MHz

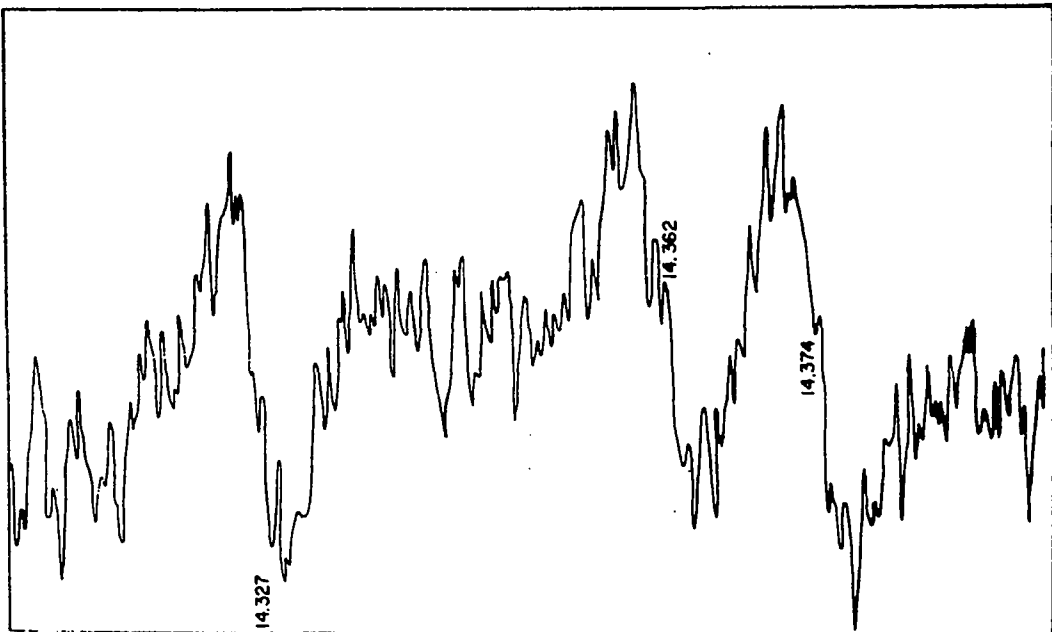


Figure 3.--Comparison of output from the Wilks superregenerative spectrometer (top) with output from the wide-line induction spectrometer (bottom).

output of the Wilks superregenerative spectrometer from a typical scan through the 14 MHz region of the nqr spectrum of  $W_2Cl_{10}$ . The shape of the spectrum appears to be indicative of a single resonance. The bottom half of the figure represents the output of the wide-line induction spectrometer from a typical scan through a small segment of the region represented in the upper trace. Uncomplicated by the presence of sidebands, the bottom output reflects the presence of three close-lying resonances rather than just one resonance as expected.

Minor modification of the Wilks system permitted temperature-dependent studies of the nqr spectrum of all of the compounds. For use with the OS-1 and OS-2 oscillators a modified coil shield was fabricated from copper and covered with Pyrex wool which permitted the passage of cold nitrogen gas (boiled from a liquid nitrogen dewar) through the sample compartments of these oscillators. In this procedure both the sample and the sample coil were cooled. A similar procedure for the OS-3 oscillator was inherently impossible because of the physical design of the oscillator. A special Pyrex tube with an evacuated jacket was designed to fit inside the sample coils of the OS-3 oscillator. Cold nitrogen gas was blown around the sample container which was mounted inside this tube. Temperatures of less than  $-100^{\circ}C$  were easily attained using

both of these gas blowing techniques. Additionally, a dewar with an unsilvered finger of appropriate outside diameter such that the finger fitted inside all of the sample coils of all three of the oscillators was designed to facilitate obtaining data at liquid nitrogen temperature.

Samples were initially sealed into Pyrex tubes of 15 mm outside diameter. The tubes were approximately six inches long and were filled to such a depth that the sample coil was completely filled with sample. The same sample tubes could be used in the modified coil shield of the OS-1 and OS-2 oscillators for temperature studies. For use in the finger dewar or the jacketed tube for the OS-3 oscillator, sample tubes of 8 mm outside diameter were required.

The temperature of a sample was easily monitored by taping the junction of a copper-constantan thermocouple onto the sample tube as close as possible to the sample coil. The electromotive force generated was measured using a Rubicon portable precision potentiometer and an ice-water ( $0^{\circ}\text{C}$ ) reference junction.

Several samples were subjected to an annealing procedure to facilitate the detection of resonances. This procedure, very similar to a procedure used for the growing of large single crystals, involved lowering the sample

in a sealed, tapered-tip sample tube through a vertically mounted tube furnace. The center of the furnace was set at a temperature conducive to complete sublimation of the material from one end of the tube to the other. This annealing procedure was especially suitable for the metal pentahalides studied because the volume of these usually fluffy materials was significantly reduced in the sample tube, thus increasing the filling factor of the sample.

Resonances were searched for by systematically scanning the full range of coils in the frequency range appropriate for the nucleus being studied. For example,  $^{35}\text{Cl}$  resonances were searched for primarily over the range 8 to 20 MHz. Such a search required two coils covering the ranges 8 to 12 and 12 to 20 MHz of the OS-1 oscillator. Twelve hours were generally required to scan the full range of each coil. Although the scan was not linear in frequency, the amount of chart paper used (usually 1.5 or 3.0 inches per hour) was linear in time, as was the motion of the calibrated knob attached to the scanning motor. For example, the start of a scan was usually set to 0 dial units (arbitrarily) and the chart recorder was marked to indicate the start of a scan; approximately 12 hours, 50 dial units, and perhaps 18 inches of chart paper later, the scan was stopped. The approximate position of any detected resonances in terms of the reading

of the knob in dial units at which the resonance occurred was determined by interpolation of the chart recording under the assumptions of linearity listed above. The resonances were then rescanned and spectrum-analyzing techniques<sup>44</sup> were used to determine the approximate frequency of the resonances.

The normal spectrum of the radio frequency (RF) output of a superregenerative oscillator as displayed on the Tektronix Model 1L20 spectrum analyzer was a central fundamental frequency pulse with less intense RF pulses equally spaced on each side of the fundamental. The fundamental was usually the strongest pulse of the spectrum and the spacing between each of the sidebands was a constant called the quench frequency. If the fundamental pulse was not immediately distinguishable, the quench frequency was varied and the fundamental pulse was presumed to be that pulse which did not move as a function of the varied quench frequency. The output from the signal generator, either a Measurements Model 80 or a Hewlett-Packard Model 608D, was also fed into the spectrum analyzer and superimposed on the spectrum of the RF output of the oscillator. When the output of the generator was precisely superimposed on the fundamental pulse of the oscillator, the frequency of the generator was measured using a Monsanto Model 110B frequency

counter. In this manner the fundamental frequency of the oscillator could easily be determined to  $\pm 10$  kHz. The strip chart recording of a resonance was very similar to the spectrum analyzer display of the output of the oscillator in that it was a central, fundamental line symmetrically surrounded by less intense sidebands. Usually in the case of a single resonance, it was possible by varying the scan rate, time constant, quench frequency, and signal gain to discern which line of the recording was the center of the resonance. To measure the frequency of this point on the recording of a resonance was fairly easy. The frequency of the oscillator was set lower than the frequency of the resonance and a scan up in frequency through the resonance was started. The pen of the recorder was carefully watched and when it reached the point of maximum deflection on the band determined to be the center or strongest band of the resonance, the scan was stopped. The fundamental frequency of the oscillator was then measured as described above. It was then assumed that since the fundamental frequency of the oscillator was the strongest pulse, it produced the strongest line in the recording of the resonance; therefore, the measured frequency of the fundamental pulse was assumed to be the frequency of the resonance. For resonances in the range 5 to 50 MHz it was possible to check these claims using

the wide-line induction spectrometer. When care was taken using spectrum analyzing techniques the agreement was usually within  $\pm 10$  kHz; when sloppy technique was used, the agreement was still usually within  $\pm 50$  kHz.

Several complications in the procedures described above occasionally arose. When two or more resonances were so close in frequency that the sidebands of one resonance overlapped with the sidebands of another resonance, the central or strongest band of the recorded spectrum was not easily discerned. In principle it should have been possible to overcome this problem using the following procedure. The resonances were recorded at least twice using different quench frequencies and the frequencies of several of the stronger bands of the spectrum were measured each time. Since the fundamental frequency was not affected by a change in the quench frequency, the bands in the spectrum which changed in frequency the least were assumed to be the resonance frequencies. Occasionally this procedure worked, but in several cases the spectrum was simply too complicated to resolve. The OS-3 oscillator had the additional problem of heating the sample. Because resonance frequencies are temperature dependent, the measurement of certain frequencies was complicated by this heating. At times the temperature of a sample in the OS-3 oscillator was 32 to 33°. Only

in certain cases could resonances in the range of the OS-3 oscillator be measured to better than  $\pm 0.1$  MHz. For resonances above approximately 180 MHz the measuring procedure had to be slightly modified because the Monsanto counter stopped working at that frequency. To eliminate this problem a Hewlett-Packard Model 10515A frequency doubler was inserted between the signal generator and the spectrum analyzer. The fundamental frequency of the generator was fed into the counter while the second harmonic was fed into the spectrum analyzer. In this manner frequency measurements up to 360 MHz were accomplished. The measurement of frequencies in the range of the OS-4 oscillator (350 to 525 MHz) was most unsatisfactory. The "trick" described above could not be used beyond 360 MHz, so internal crystal calibration of the Hewlett-Packard signal generator had to be relied upon. The only calibration possible was at integral multiples of 1 or 5 MHz. Additionally, the high end of the range of this generator was 400 MHz meaning that it was again necessary to use the frequency doubler beyond 400 MHz. That meant the calibration of the second harmonic was only possible at integral multiples of 2 or 10 MHz. As a result, resonances in the range of the OS-4 oscillator could only be measured to  $\pm 1.0$  MHz.

Corresponding  $^{37}\text{Cl}$  and  $^{79}\text{Br}$  resonances were

detected for all new  $^{35}\text{Cl}$  and  $^{81}\text{Br}$  resonances listed in Tables III, IV, and V of Assignment of Resonances section of this thesis. The values for the ratio of the quadrupole moments for the alternate isotopes of nuclei under investigation were obtained from Segel and Barnes.<sup>45</sup>

Numerical Interpretation of Data.--Most interpretive procedures were simple enough not to require computer assistance. However, several small programs were locally written using the local Conversational Programming Service (CPS) option and executed by teletype link-up with the IEM-360-75 computer. A few programs were written in FORTRAN IV G. The important programs alluded to in the following sections of this thesis are described further in the Appendix.

## ASSIGNMENT OF RESONANCES

Niobium Pentahalides. --The experimental results for all of the niobium pentahalides are listed in Table III. It was not possible to reproduce the nqr results of Reddoch<sup>5</sup> in  $\text{Nb}_2\text{Cl}_{10}$  without annealing the sample. The sample of  $\text{Nb}_2\text{Br}_{10}$  used in this study was similarly annealed and the results of Busl'aev *et al.*<sup>10</sup> were also reproduced. The sample of  $\text{Nb}_2\text{I}_{10}$  was not annealed. The assignment of the  $^{93}\text{Nb}$  resonances in  $\text{Nb}_2\text{Br}_{10}$  is clear despite the fact only two of the four possible resonances were detected. Because no signals were detected at higher frequencies, the 9.891 and 7.270 MHz resonances are assigned as the  $\pm 7/2 \leftrightarrow \pm 9/2$  and  $\pm 5/2 \leftrightarrow \pm 7/2$  transitions respectively. This assignment requires the other allowed transitions to fall in the range 4.5 to 5.0 MHz, but this could not be verified because those frequencies were below the operating range of our spectrometer systems. The value for the asymmetry parameter (obtained using Cohen's tables<sup>33</sup>),  $\eta = 0.40$ , also corresponds well to that exhibited by  $^{93}\text{Nb}$  in  $\text{Nb}_2\text{Cl}_{10}$ ,  $\eta = 0.32$ . Because the  $^{93}\text{Nb}$  resonances in  $\text{Nb}_2\text{Br}_{10}$  are at lower frequencies than those in  $\text{Nb}_2\text{Cl}_{10}$ , and because repeated scans from 5 to 20 MHz revealed no resonances in  $\text{Nb}_2\text{I}_{10}$ , it is presumed all  $^{93}\text{Nb}$  resonances in  $\text{Nb}_2\text{I}_{10}$  are at frequencies less than 5 MHz. The  $^{127}\text{I}$  resonances in  $\text{Nb}_2\text{I}_{10}$  are also

Table III

## Experimental Results for Niobium Pentahalides

Cmpd	Isotope	T, °C	$\nu_{\text{terminal}}$ (MHz)	$\nu_{\text{bridge}}$ (MHz)	$\nu_{\text{metal}}$ (MHz)		Extracted parameters		Reference	
					Observed	Calcd	( $e^2 Q q / h$ )	$\eta$		
Nb <sub>2</sub> Cl <sub>10</sub>	<sup>35</sup> Cl	24.5		13.06					5	
		-196		13.28						
	<sup>93</sup> Nb	24.5				$\nu_1$	5.423	5.423	78.08	0.32
						$\nu_2$	6.062	6.062		
						$\nu_3$	9.561	9.561		
						$\nu_4$	12.903	12.903		
	<sup>93</sup> Nb	-196				$\nu_1$	5.715	5.715	78.26	0.35
						$\nu_2$	6.052	6.051		
					$\nu_3$	9.547	9.547			
					$\nu_4$	12.913	12.913			
Nb <sub>2</sub> Br <sub>10</sub>	<sup>81</sup> Br	27	50.53	87.96					10	
			52.11	88.39						
				89.07						
	Br	-196	49.43	89.37						
			49.95	89.83						
				90.25						

Table III (continued)

Cmpd	Isotope	T, °C	$\nu_{\text{terminal}}$ (MHz)	$\nu_{\text{bridge}}$ (MHz)	$\nu_{\text{metal}}$ (MHz)		Extracted parameters		Reference	
					Observed	Calcd	( $e^2 Qq/h$ )	$\eta$		
Nb <sub>2</sub> Br <sub>10</sub>	<sup>93</sup> Nb	ca. 24			$\nu_3$	7.270	7.270 <sup>a</sup>	60.01	0.40	This work
					$\nu_4$	9.891	9.891 <sup>a</sup>			
Nb <sub>2</sub> I <sub>10</sub>	<sup>127</sup> I	R.T. <sup>b</sup>	$\nu_1$	49.55	118. <sup>c</sup>			Ter.		This work
			$\nu_1$	50.26				327.6	0.14	
			$\nu_2$	96.56				323.2	0.15	
			$\nu_2$	97.87		185. <sup>c</sup>		Bridge		
	<sup>127</sup> I	-196	$\nu_1$	48.69				Ter.		
			$\nu_1$	49.60	119. <sup>c</sup>			313.4	0.18	
			$\nu_2$	93.43			314.9	0.22		
			$\nu_2$	93.63	188. <sup>c</sup>		Bridge			
							655.	0.47		

<sup>a</sup>Calculated using a locally written CPS program (F92,PAE). See Appendix.

<sup>b</sup>Not all data taken at same temperature. <sup>c</sup>Possibly multiple resonances too close together to resolve.

easy to assign. Using either the criterion of a positive temperature coefficient indicative of a terminal halogen atom resonance as suggested by Buslaev *et al.*,<sup>10</sup> or the criterion of a large asymmetry parameter indicative of a bridging halogen atom resonance as found in the group IIIA trihalides,<sup>14,15</sup> the assignment is the same. The resonances at higher frequencies are assigned to the bridging halogen atoms while the resonances at lower frequencies are assigned to the terminal halogen atoms.

Tantalum Pentahalides. --The experimental results for all of the tantalum pentahalides are listed in Table IV. The room temperature  $^{35}\text{Cl}$  nqr results of Safin *et al.*<sup>7</sup> were reproduced and  $^{181}\text{Ta}$  resonances were detected using an annealed sample of  $\text{Ta}_2\text{Cl}_{10}$ . The room temperature Br nqr results of Buslaev *et al.*<sup>10</sup> were confirmed using an unannealed sample of  $\text{Ta}_2\text{Br}_{10}$ , but an annealed sample was used for the  $^{181}\text{Ta}$  study. Extra Br resonances very close in frequency to those reported by Buslaev *et al.*<sup>10</sup> were also detected in the annealed sample. The frequencies of these resonances were not measured because this change of multiplicity of resonances did not change the assignment of the detected resonances. It is, however, a "textbook" demonstration of the impact of subtle crystal effects on the multiplicity of resonances of chemically equivalent nuclei. The sample of  $\text{Ta}_2\text{I}_{10}$  used was not annealed.

Table IV  
Experimental Results for Tantalum Pentahalides

Cmpd	Isotope	T, °C	$\nu_{\text{terminal}}$ (MHz)	$\nu_{\text{bridge}}$ (MHz)	$\nu_{\text{metal}}$ (MHz)	Extracted parameters		Reference
						( $e^2Qq/h$ )	$\eta$	
Ta <sub>2</sub> Cl <sub>10</sub>	<sup>35</sup> Cl	20			13.35			7
					13.37			
					13.39			
		-196	12.30 (mean of doublet)	13.6 (mean of triplet)				
	<sup>181</sup> Ta	R.T. <sup>a</sup>			$\nu_1$ 177.6	1786.	0.36	This work
				$\nu_1$ 183.0				
				$\nu_2$ 241.4	1795.			
Ta <sub>2</sub> Br <sub>10</sub>	<sup>81</sup> Br	27	54.98	90.30				10
			55.30					
			56.59					
		-196	54.18	91.48				
			54.27					
			54.50					
			54.97					

<sup>a</sup>Not all data taken at same temperature.

Table IV (continued)

Cmpd	Isotope	T, °C	$\nu_{\text{terminal}}$ (MHz)	$\nu_{\text{bridge}}$ (MHz)	$\nu_{\text{metal}}$ (MHz)	Extracted parameters		Reference
						( $e^2Qq/h$ )	$\eta$	
$\text{Ta}_2\text{Br}_{10}$	$^{181}\text{Ta}$	R.T. <sup>a</sup>			$\nu_1$ 156.7	1421.	0.45	This work
					$\nu_1$ 161.1	1436.	0.46	
					$\nu_2$ 190.0			
$\text{Ta}_2\text{I}_{10}$	$^{127}\text{I}$	R.T. <sup>a</sup>	$\nu_1$ 71.98	$\nu_1$ 123.3		Ter.		This work
			$\nu_1$ 72.69			478.0	0.06	
			$\nu_2$ 143.3	$\nu_2$ 211.6		482.6	0.06	
			$\nu_2$ 144.6			Bridge		
						723.2	0.37	
	$^{181}\text{Ta}$	R.T. <sup>a</sup>			$\nu_1$ 87.4	861.	0.38	
					$\nu_2$ 116.3	870.	0.37	
					$\nu_2$ 117.3			

To the author's knowledge the  $^{181}\text{Ta}$  resonances listed in Table IV are the first nqr resonances reported for this nucleus. Unfortunately, since only two of the three allowed transitions for an  $I = 7/2$  nucleus (such as  $^{181}\text{Ta}$ ) have been detected, the assignment of the resonances as shown in the table is open to question. Scans from 100 to 350 MHz yielded no other resonances in  $\text{Ta}_2\text{Cl}_{10}$  or  $\text{Ta}_2\text{Br}_{10}$  not otherwise accounted for. Other potential assignments require the third transition to be in the frequency range scanned, and/or yield values of  $\eta$  much greater than reasonable when compared to values of  $\eta$  exhibited by  $^{93}\text{Nb}$  in  $\text{Nb}_2\text{Cl}_{10}$  or  $\text{Nb}_2\text{Br}_{10}$ . In fact, a third transition for  $^{181}\text{Ta}$  in  $\text{Ta}_2\text{Br}_{10}$  is required by the assignment shown in the table to fall in the range 300 to 350 MHz. It could be rationalized that this resonance was not detected because the OS-3 oscillator was not as sensitive as desirable at the high end of its range and/or because the probability of the third transition, according to Cohen,<sup>33</sup> is less than those of the two lower transitions. However, these assignments can only be affirmed by the detection of those third transitions and, hopefully, when the OS-4 oscillator has been fully developed, these transitions will be found. Because it is hard to conceive of Cl or Br resonances falling in the range of 200 MHz in these compounds, these resonances are interpreted as  $^{181}\text{Ta}$  resonances.

The assignment of resonances detected in  $\text{Ta}_2\text{I}_{10}$  is not quite so clear-cut because the  $^{127}\text{I}$  and  $^{181}\text{Ta}$  resonances in this compound could fall in the same frequency range. The assignment shown in Table IV is based on the following arguments. In the group VB metal pentachlorides and pentabromides, the halogen resonances in the tantalum compounds are all at higher frequencies than in the corresponding niobium compounds. The temperature dependence of the resonances was considered as was the magnitude of the asymmetry parameters implied by each potential assignment. The assignment of the terminal halogen atom resonances appears clear because the 72 and 144 MHz resonances exhibit positive temperature coefficients, the asymmetry parameter implied by this assignment is small, and each "set" of resonances is a pair of close-lying resonances at room and liquid nitrogen temperatures. The assignment of the  $\nu_2$  bridging halogen resonance also appears straightforward because it exhibits a negative temperature coefficient. From this point on the assignment is extremely tenuous and based in part on the elimination of other possible assignments. It should be noted that the 87.4 MHz resonance exhibits a positive temperature coefficient and at reduced temperatures it splits into two close-lying resonances. The 116.3 and 117.3 MHz resonances also exhibit positive temperature coefficients, while the temperature

coefficient of the 123.3 MHz resonance is unclear. At liquid nitrogen temperature this latter resonance splits into two resonances which are too close in frequency to be objectively separated and assigned frequencies. The temperature dependence of this "array" of resonances is, however, very small. At liquid nitrogen temperature each of the two resonances is probably within 0.5 MHz of 123.3 MHz. Thus several other assignments of terminal halogen atom resonances appear possible. For example, the 72 MHz resonances, as  $\nu_1$ , could be associated with the 116 or 123 MHz resonances, as  $\nu_2$ ; and the 87.4 MHz resonance, as  $\nu_1$ , could be associated with the 123 or 144 MHz resonances, as  $\nu_2$ . However any assignment which breaks the association of the 72 and 144 MHz resonances implies a value of  $\eta$  in the range 0.35 to 0.50 for a terminal halogen atom. A value of  $\eta$  of this magnitude is very hard to rationalize, especially in comparison to the values of  $\eta$  exhibited by terminal  $^{127}\text{I}$  atoms in  $\text{Nb}_2\text{I}_{10}$ . Next, at issue is which of the 116 or 123 MHz resonances should be assigned as  $\nu_1$  for a bridging halogen atom, and how should the remaining two sets of resonances be assigned. The 123.3 MHz resonance is assigned as the  $\nu_1$  bridging halogen atom resonance because such an assignment implies a value for  $\eta$  closest to that exhibited by bridging  $^{127}\text{I}$  atoms in  $\text{Nb}_2\text{I}_{10}$ . The remaining unassigned resonances are those at 87.4 MHz

and the doublet near 116 MHz. If these resonances are  $^{127}\text{I}$  resonances, values of  $\eta$  greater than 0.65 are implied. Such values are too large to be associated with terminal halogen atoms and the frequencies themselves are too low to be indicative of bridging halogen atoms. However, if these resonances are assigned as  $^{181}\text{Ta}$  resonances,  $\nu_1$  and  $\nu_2$  respectively, values of  $\eta$  on the order of 0.37 are implied. Such a value for  $\eta$  compares well with those exhibited by the metal nuclei in  $\text{Nb}_2\text{Cl}_{10}$ ,  $\text{Ta}_2\text{Cl}_{10}$ ,  $\text{Nb}_2\text{Br}_{10}$ , and  $\text{Ta}_2\text{Br}_{10}$ . Unfortunately, this assignment requires the third  $^{181}\text{Ta}$  transitions to be at frequencies at which no resonances have been detected. The lower transition probability of the third transition serves as a convenient rationalization for the lack of detection of those resonances. Clearly, the assignment of the resonances in  $\text{Ta}_2\text{I}_{10}$  is open to debate.

Related Metal Pentahalides.--The experimental results for the other related metal pentahalides are listed in Table V. The assignments shown in the table are again based primarily on the sign of the temperature coefficient,  $d\nu/dT$ . As suggested by Buslaev *et al.*<sup>10</sup> a negative  $d\nu/dT$  was assumed to be indicative of a bridging halogen atom resonance while a positive  $d\nu/dT$  was assumed to be indicative of a terminal halogen atom resonance. It is interesting to note the multiplicity of the

Table V

## Experimental Results for Related Metal Pentahalides

Cmpd	Isotope	T, °C	$\nu_{\text{terminal}}$ (MHz)	$\nu_{\text{bridge}}$ (MHz)	Sign of $d\nu/dT$	Reference
Mo <sub>2</sub> Cl <sub>10</sub>	<sup>35</sup> Cl	32		14.085	Negative	18
W <sub>2</sub> Cl <sub>10</sub>	<sup>35</sup> Cl	ca. 24		14.374 14.362 14.327	Negative	This work
			12.226 9.444 9.371 9.254		ca. 0 Positive	
W <sub>2</sub> Br <sub>10</sub>	<sup>81</sup> Br	R.T.	72.24	95.68	Negative <sup>a</sup> Positive <sup>a</sup>	This work
		-196	75.58 76.34	96.57		
Re <sub>2</sub> Cl <sub>10</sub>	<sup>35</sup> Cl	ca. 24		17.318 17.104 16.387 16.312	Negative	This work
			15.891 15.731 13.291 13.277 13.203 13.155		Positive	

<sup>a</sup>Over the range R.T. to -110°.

terminal resonances, for example, varies from compound to compound and appears to bear little correlation to the similar dimeric structure of the compounds. In the same vein, the lack of terminal halogen nqr data for yet another compound ( $\text{Mo}_2\text{Cl}_{10}$ ) continues to defy explanation.

The results for  $\text{W}_2\text{Cl}_{10}$  are not easy to correlate with the dimeric structure of the compound.<sup>46</sup> The detection of three distinct groups of  $^{35}\text{Cl}$  resonances does not correlate with the two types of halogen atoms present in the molecule, especially when the number of resonances in each group is considered. Three samples of  $\text{W}_2\text{Cl}_{10}$ , each physically treated differently, exhibited the same number of resonances. The first sample, which was annealed, was probably contaminated by the presence of a tungsten oxychloride. A band in the region of  $900\text{ cm}^{-1}$  in the far infrared spectrum of the sample, assignable as a W-O stretching band, indicated the presence of the impurity. The tungsten oxychloride was sublimed away from the  $\text{W}_2\text{Cl}_{10}$  almost quantitatively as indicated by the disappearance of the W-O stretching band. An unannealed sample of the purified  $\text{W}_2\text{Cl}_{10}$  and an unannealed sample of the impure  $\text{W}_2\text{Cl}_{10}$  exhibited all of the resonances detected in the original sample. Therefore, it is concluded that each of the resonances is "real" and should be considered part of the nqr spectrum of  $\text{W}_2\text{Cl}_{10}$ .

The interpretation of the experimental results for  $W_2Br_{10}$  is complicated by a different problem. It should be noted the sample of  $W_2Br_{10}$  used in this study was not annealed. The temperature coefficients of the bridging and terminal halogen atom resonances over the range 30 to  $-110^\circ$  are negative and positive, respectively, as expected. However, at  $-196^\circ$  the terminal halogen atom resonance splits into two resonances, both of which are at frequencies higher than the room temperature resonance; i.e., the sign of the temperature coefficient has changed from positive to negative. Such a change in the sign of  $d\nu/dT$  is not easy to interpret, particularly without additional frequency measurements made at temperatures between  $-110$  and  $-196^\circ$ . If a sharp break in the almost linear temperature dependence had been detected, it would have been strong evidence for the presence of a phase transition at the temperature at which the break occurred. However, a more gradual change in the sign of  $d\nu/dT$ , as evidenced by a plot of frequency vs. temperature in which the frequency goes through a minimum as in the case of  $W_2Br_{10}$  or goes through a maximum as in the case of the Br resonances in  $TiBr_4$  as detected by Barnes and Engardt,<sup>47</sup> would have been strong evidence for more subtle changes in bonding. These changes could either be intermolecular as suggested by Barnes and Engardt<sup>47</sup> or intramolecular as

suggested by Reddoch.<sup>5</sup> As mentioned earlier, without additional data any speculation as to the actual mechanism leading to the unusual temperature dependence exhibited by the terminal Br atom resonances in  $W_2Br_{10}$  would be imprudent.

The experimental results for  $Re_2Cl_{10}$  appear at first glance to be the easiest to interpret in relation to the known dimeric structure<sup>48</sup> of the compound. The coincidence of 10 detected  $^{35}Cl$  resonances and 10 Cl atoms per molecule of dimer appears convenient, but the fact that 4 of these resonances exhibit temperature coefficients indicative of bridging halogen atom resonances destroys that convenience. Although both  $Re_2Cl_{10}$  and  $Nb_2Cl_{10}$  are dimeric, and structurally approximated as two octahedra sharing an edge, there are significant differences in their respective structures because the two compounds are not isomorphous. The symmetry of the unit cell of  $Re_2Cl_{10}$ ,  $P2_1/c$ , requires the four molecules in the unit cell to be equivalent. The symmetry of each molecule almost contains three mutually perpendicular mirror planes, although no symmetry is required. Thus 10  $^{35}Cl$  resonances, one from each Cl atom in the dimeric unit, would be expected in the nqr spectrum of  $Re_2Cl_{10}$ . It is possible, that two terminal Cl atoms inexplicably exhibit negative rather than positive temperature coefficients. In fact, the

magnitude of the temperature coefficients associated with the 16 MHz resonances is approximately half as large as those of the 17 MHz resonances. The assignment of the 16 MHz resonances must then be considered as suspect. One safe conclusion would appear to be that crystal effects play a significant role in the nqr spectrum of  $\text{Re}_2\text{Cl}_{10}$ . The lack of detection of any resonances assignable as  $^{185}\text{Re}$  or  $^{187}\text{Re}$  transitions is another disappointing aspect of the nqr study of  $\text{Re}_2\text{Cl}_{10}$ .

## INTERPRETATION

Interpretation of Metal Resonances.--In order to interpret the  $^{93}\text{Nb}$  and  $^{181}\text{Ta}$  data, values for the asymmetry parameter and the quadrupole coupling constant were calculated from the observed resonance frequencies. Values for the field gradient were extracted from the quadrupole coupling constant using values for the quadrupole moments of  $^{93}\text{Nb}$  and  $^{181}\text{Ta}$ , equal to  $-0.20$  and  $3.9$  barns respectively, as given by Korol'kov and Makhanev.<sup>49</sup> The values for  $\eta$  and  $e^2Qq/h$  exhibited by  $^{93}\text{Nb}$  in  $\text{Nb}_2\text{Cl}_{10}$  were taken from Reddoch.<sup>5</sup> In the case of  $\text{Nb}_2\text{Br}_{10}$ ,  $\eta$  was obtained using Cohen's tables,<sup>33</sup> and  $e^2Qq/h$  was obtained by two different methods. First it was determined using  $\eta$  and the two equations for  $\nu_3$  and  $\nu_4$  given in Table II with the aid of a locally written CPS program (F92,PAE) (see Appendix); and second, it was determined using Cohen's tables.<sup>33</sup> The close correspondence between the two inferred values,  $60.14$  MHz using the first method, and  $60.01$  MHz using the second method, is quite good. The first method, is reliable only because the two equations used are the last of the four equations for the  $I = 9/2$  spin case to break down for large values of  $\eta$ . A similar procedure for the determination of the parameters exhibited by  $^{181}\text{Ta}$  in  $\text{Ta}_2\text{Cl}_{10}$ ,  $\text{Ta}_2\text{Br}_{10}$ , and  $\text{Ta}_2\text{I}_{10}$  gives less satisfactory results. The values for  $\eta$  should be reliable, but the

values for  $e^2 Qq/h$  obtained using the two different methods differ by as much as 40 MHz. The equations for the observed transitions,  $\nu_1$  and  $\nu_2$ , are the most sensitive to changes in  $\eta$  and, hence, are the least reliable of the three equations for the  $I = 7/2$  spin case for large values of  $\eta$ . The values of  $e^2 Qq/h$  given in Tables III and IV were obtained using Cohen's tables.<sup>33</sup> The extracted values for the field gradient (eq) exhibited by the metal in the five group VB metal pentahalide dimers studied are listed in Table VI. The quantity  $f_{<} / f_{>}$  also listed in Table VI will be explained later.

It is seemingly paradoxical that the value of eq exhibited by a given metal decreases as the halogen is varied from Cl to Br to I. (The field gradient for  $^{93}\text{Nb}$  in  $\text{Nb}_2\text{I}_{10}$  must be assumed to be less than that detected in  $\text{Nb}_2\text{Br}_{10}$  because all of the Nb resonances in that compound have been assumed to be at frequencies less than 5 MHz.) The opposite trend would have been predicted on the basis of the increased covalency of a single metal-halogen bond. Because  $\text{Nb}^{5+}$  is formally a  $d^0$  ion, any field gradient should be the result of the population of electrons rather than electron holes. One might assume that as the halogen becomes less electronegative the number of electrons on the metal should increase, thus increasing the effective field gradient of the metal. This line of reasoning has

Table VI

Metal Field Gradients and Ratios of  
Force Constants in  $M_2X_{10}$

Cmpd	Metal field gradient (esu/cm <sup>3</sup> )	$f_{<} / f_{>}$
Nb <sub>2</sub> Cl <sub>10</sub>	5.39 x 10 <sup>15</sup>	0.380 ± 0.043
Nb <sub>2</sub> Br <sub>10</sub>	4.14 x 10 <sup>15</sup>	0.563 ± 0.097
Ta <sub>2</sub> Cl <sub>10</sub>	6.32 x 10 <sup>15</sup>	0.335 ± 0.012
	6.35 x 10 <sup>15</sup>	
Ta <sub>2</sub> Br <sub>10</sub>	5.03 x 10 <sup>15</sup>	0.511 ± 0.014
	5.08 x 10 <sup>15</sup>	
Ta <sub>2</sub> I <sub>10</sub>	3.08 x 10 <sup>15</sup>	0.825
	3.05 x 10 <sup>15</sup>	

one major flaw in it. The effective field gradient is also a function of the orientation of the six bonding tensors representing the six  $\sigma$ -bonds in which the metal is participating. If each of these tensors were of equal magnitude and pointed directly toward the corner of a regular octahedron, the effective field gradient around the metal at the center of that octahedron would be zero regardless of the magnitudes of those tensors. The implication of the trend toward smaller values of eq is that the environment around the metal atom more closely approaches octahedral symmetry as the halogen is varied from Cl to Br to I.

A normal coordinate analysis of  $M_2X_{10}$  compounds was performed by Dr. Richard Smardzewski<sup>42</sup> of this laboratory. Values for axial, equatorial, and bridging M-X stretching force constants were determined during that study. A quantity of interest in that study was the ratio of the bridging to the equatorial stretching force constant. The quantity of interest in interpreting field gradients should not be dependent upon whether the vibration involved is a bridging or terminal vibration; only the magnitudes of the force constants should be germane. Thus the quantity  $f_{<} / f_{>}$  is the ratio of the smaller to the larger of the two force constants. Significantly, the bridging and terminal force constants become more similar as the halogen is varied from Cl to Br to I. Figure 4 shows a plot of

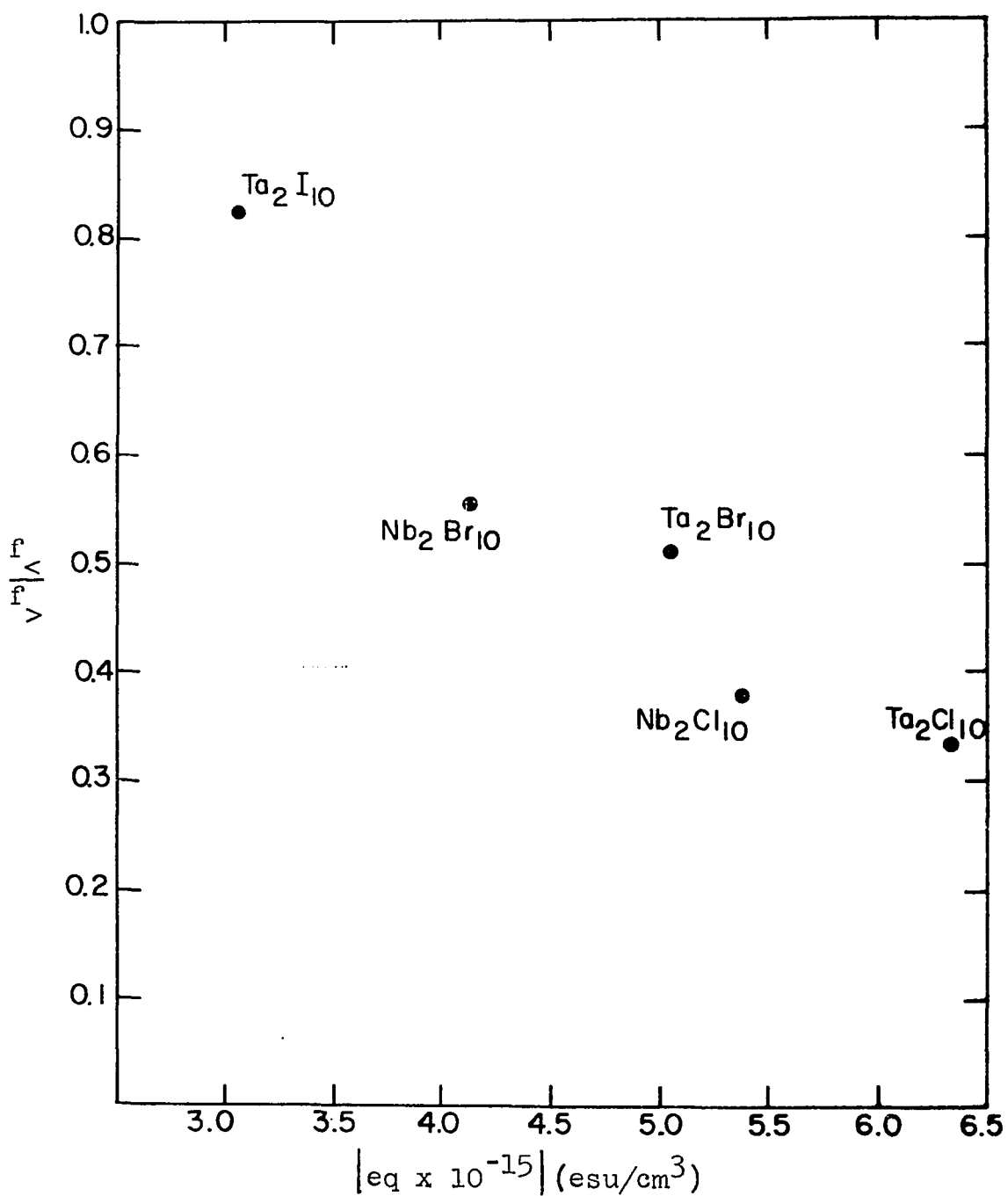


Figure 4. Plot of ratio of force constants vs. metal field gradients in  $M_2X_{10}$ .

$f_{<}/f_{>}$  as the ordinate vs.  $\nu_{eq}$  as the abscissa. This plot clearly demonstrates the correlation between the two quantities and is support for the claim that the metal is more closely approaching octahedral symmetry as the halogen is varied from Cl to Br to I. Similarly, this correlation should be affirmation of Dr. Smardzewski's suggestion "that halogen bridge bonding becomes energetically favorable in the order  $I > Br > Cl$  for the heavy transition metal halides."

Interpretation of Halogen Resonances.--The interpretation of the halogen resonances is very difficult for several reasons. Consider, for example, the results for the terminal halogen atoms in  $Re_2Cl_{10}$  and  $W_2Cl_{10}$ . It appears imprudent to attempt to "interpret" these resonances because it is hard to even explain their multiplicities. Consider also the results in  $Nb_2Cl_{10}$  and  $Mo_2Cl_{10}$ . How can the results for the terminal halogen atom resonances in those compounds be properly interpreted when no terminal halogen atom resonances have been detected? Indeed, how can the fact that no terminal halogen atom resonances were observed be rationalized? In this respect, the results of this study are most unsatisfactory.

Two general comments about the terminal halogen atom resonances do, however, seem appropriate. First, it does appear that the terminal halogen atoms in these dimeric

compounds do donate some electron density into empty metal d orbitals via a  $\pi$ -bond. This conclusion is based on the positive temperature coefficients exhibited by the terminal halogen atom resonances in accordance with the suggestions made by Buslaev and co-workers.<sup>10</sup> However, the magnitude of the  $\pi$  interaction is very hard to estimate. Second, there does appear to be a general trend toward higher terminal halogen atom resonance frequencies as the metal is changed from a member of group VB to VIB to VIIB. For the resonance frequency of a  $\pi$ -bonded terminal halogen atom to increase, the absolute magnitude of the difference between the populations of the  $\sigma$ - and  $\pi$ -bonded orbitals must increase. It must be remembered that it is assumed the population of the  $\pi$ -bonding halogen orbitals is only slightly less than 2. Thus, either an increase in the covalency of the M-X  $\sigma$ -bond (lowering the  $\sigma$  population on the halogen atom) or a decrease in the covalency of the M-X  $\pi$ -bond (raising the  $\pi$  population on the halogen atom) leads to an increase in the absolute magnitude of the difference between the two populations. Both mechanisms are probably operative. First, the electronegativity difference between metal and halogen decreases as the metal is varied from group VB to VIIB providing a potentially more covalent  $\sigma$ -bond. Second, as the metal is varied from

group VB to VIIB the metal d orbitals become more populated with metal electrons thus reducing the ability of the halogen to donate electron density to the metal. These two mechanisms do not appear easily separable.

Fortunately, a little more can be said quantitatively about the bridging halogen atom resonances. The coordinate system and equations used to interpret the bridging halogen atom resonances will be as given by Lucken,<sup>31</sup> and are listed on pages 26, 29, and 30 of this thesis. The wavefunctions used for the hybrid orbitals are given in equation (17). Equations (25) and (26) relate the molecular quadrupole coupling constant ( $e^2Qq_{mol}$ ) and the asymmetry parameter to the  $M-X_b-M$  angle and the population of the  $\sigma$ -bonding hybrid orbital on the halogen atom, and equation (22) is used to relate the populations of the hybrid orbitals to the populations of the pure atomic orbitals. The values of the atomic coupling constants ( $e^2Qq_{atm}$ ) used in these computations for  $^{35}\text{Cl}$ ,  $^{81}\text{Br}$ , and  $^{127}\text{I}$ , as taken from Townes and Schawlow,<sup>50</sup> are 109.7, -643.1, and 2292.8 MHz respectively. It is possible to predict the  $M-X_b-M$  angle in the case of  $^{127}\text{I}$  containing compounds because  $\eta$  can be experimentally determined, while conversely, because  $\eta$  cannot be explicitly determined in the case of  $^{35}\text{Cl}$  and  $^{81}\text{Br}$  containing compounds, known or assumed structural data<sup>42</sup> are used to predict

values for  $\eta$ . The results of these numerical calculations are shown in Table VII. The  $^{35}\text{Cl}$  and  $^{81}\text{Br}$  data were analyzed with the aid of a locally written CPS program (BHR, PAE) (see Appendix). Three important conclusions can be drawn from the data presented in the table. First, the  $\text{M-X}_b\text{-M}$  angles inferred from experimental results for  $\text{Nb}_2\text{I}_{10}$  and  $\text{Ta}_2\text{I}_{10}$  correspond well to those angles determined by single crystal X-ray diffraction studies of  $\text{Nb}_2\text{Cl}_{10}$ ,  $\text{Mo}_2\text{Cl}_{10}$ , and  $\text{Re}_2\text{Cl}_{10}$ . All angles whether determined by nqr or X-ray diffraction studies fall in the range  $97$  to  $102^\circ$ . This is particularly noteworthy because the angle determined by nqr is most correctly the angle between regions of high electron density arising from the hybrid orbitals and need not necessarily correspond to the angle between atom-center-to-atom-center vectors as determined by crystallographic studies. Said differently, the possibility of "bent" or "banana" bonding does exist; but based on the close correlation between nqr and crystallographically determined bond angles, it does not appear necessary to invoke such bonding in these compounds. Second, there appears to be a trend toward smaller  $\text{M-X}_b\text{-M}$  angles as the halogen is varied from Cl to Br to I. This is not surprising because the hybridization energy for I is greater than for Cl. Thus, the amount of s character in the hybrid orbitals and in turn the interorbital angle

Table VII  
Interpretation of Bridging Halogen Atom Resonances

Cmpd	Nucleus	M-X <sub>p</sub> -M angle	ν <sub>Q</sub> (MHz)	Calculated parameters			
				e <sup>2</sup> Qq/h	η	B	N <sub>t</sub>
Nb <sub>2</sub> Cl <sub>10</sub>	<sup>35</sup> Cl	101.3	13.058	24.731	0.588	1.73	7.46
Ta <sub>2</sub> Cl <sub>10</sub>	<sup>35</sup> Cl	101.3	13.35	25.284	0.588	1.72	7.45
Mo <sub>2</sub> Cl <sub>10</sub>	<sup>35</sup> Cl	98.6	14.08	27.260	0.449	1.71	7.43
W <sub>2</sub> Cl <sub>10</sub>	<sup>35</sup> Cl	98.6	14.327	27.739	0.449	1.71	7.42
			14.361	27.805		1.71	7.42
			14.373	27.828		1.71	7.42
Re <sub>2</sub> Cl <sub>10</sub>	<sup>35</sup> Cl	98.74	17.318	33.495	0.456	1.65	7.30
			17.104	33.081		1.65	7.31
			16.387	31.695		1.67	7.33
			16.312	31.625		1.67	7.34
Nb <sub>2</sub> Br <sub>10</sub>	<sup>81</sup> Br	101.3	88.39	167.40	0.588	1.69	7.38
Ta <sub>2</sub> Br <sub>10</sub>	<sup>81</sup> Br	101.3	90.30	171.02	0.588	1.68	7.36
W <sub>2</sub> Br <sub>10</sub>	<sup>81</sup> Br	98.6	95.68	185.25	0.449	1.67	7.34
Nb <sub>2</sub> I <sub>10</sub>	<sup>127</sup> I	99.	118. 185.	642.	0.48	1.69	7.38
Ta <sub>2</sub> I <sub>10</sub>	<sup>127</sup> I	97.	123.3 211.6	722.	0.37	1.65	7.30

would be expected to decrease in the order shown. Additionally, a larger halogen, such as I, would tend to minimize repulsive interactions between the formally positively charged Nb atoms. In the case of  $\text{Nb}_2\text{Cl}_{10}$  these repulsive interactions lead to a surprisingly large  $\text{M-X}_b\text{-M}$  angle because the Nb atoms are situated in positions distorted from octahedral holes with greater M-M distances than would be found if the Nb atoms were in octahedral holes. A larger halogen would lessen these repulsive interactions thus leading to a smaller bridging angle. Third, a general trend toward more covalent  $\text{M-X}_b\text{-M}$  binding is apparent both as the atomic number of the metal atom is increased, and as the atomic number of the halogen atom is increased. A similar trend was inferred from the terminal halogen atom data.

## SUMMARY

A summary of the individual trends previously discussed presents a relatively satisfying description of the bonding in the metal pentahalide dimers. First, the terminal halogen atoms donate electron density into empty metal d orbitals via a  $\pi$  type interaction. Second, the bridging halogen atoms  $\sigma$ -bond to the metal atoms making use of hybrid orbitals composed of s,  $p_x$ , and  $p_y$  atomic orbitals. Third, bridging and possibly terminal halogen atoms become more covalently bound to the metal atom as the size of the halogen atom and metal atom is increased. Fourth, the environment of the metal atom becomes more octahedral in nature as the size of the halogen atom is increased.

## SUGGESTIONS FOR FUTURE WORK

There are many avenues of potential research that stem from this thesis. One or more of these will probably have been initiated by the time this thesis has been officially submitted.

An nqr study of both the metal and halogen atoms in acetonitrile adducts of niobium and tantalum pentahalides,  $MX_5L$ , could aid in understanding the bonding in these compounds. Of particular interest would be the variation of the field gradient of the metal as a function of both the halogen and the metal involved in the compound. Work along this line has already been initiated.

The use of nqr to detect the presence of bridging and terminal halogen atoms in compounds of unknown structure is an obvious extension of this thesis. The compound  $Nb_2Br_6(SC_4H_8)_3$  is already being studied with this goal in mind. It is an obvious starting point because the nqr results will be comparable to the results of a single crystal X-ray diffraction study of the compound presently under way.

Research more closely related to the results of this study would center on the significance of lattice contributions to the field gradient of a halogen atom in an  $M_2X_{10}$  compound. The variation in the number of halogen atom resonances detected in each of the studied compounds

suggests that such contributions could be more significant than assumed in this thesis. A study of the pressure dependence of nqr transitions in a compound of known structure could clarify the importance of these lattice contributions.  $\text{Re}_2\text{Cl}_{10}$  would appear to be the logical choice for such a study because it is the only  $\text{M}_2\text{X}_{10}$  compound of known structure in which both terminal and bridging halogen atom resonances were detected.

A temperature dependent study of the electron spin resonance (esr) spectrum and the magnetic susceptibility should be made of  $\text{W}_2\text{Br}_{10}$ .  $\text{W}^{5+}$  is a  $d^1$  ion and  $\text{W}_2\text{Br}_{10}$  is known to be paramagnetic.<sup>51</sup> One possible explanation not discussed earlier for the strange temperature dependence exhibited by the Br nqr resonances in this compound could be that the molecule as a whole undergoes a transition from the  $S = 1$  to the  $S = 0$  state at low temperature. There is no reason to assume that the field gradients of the Br nuclei in the two states should be the same. Such a transformation should be easy to detect either by esr or magnetic susceptibility studies.

A study of nqr transitions of metal nuclei could also be a probe into the extent of metal-metal bonding in heavy transition metal compounds. The field gradient of the metal atom would almost certainly be affected by the presence of strong metal-metal interactions. In fact,

one possible explanation for the large field gradient exhibited by  $^{93}\text{Nb}$  in  $[(\text{CH}_3)_4\text{N}]_2[(\text{Nb}_6\text{Cl}_{12})\text{Cl}_6]$  could be the presence of such interactions. A study of compounds of known structure in which such interactions are thought to be present could lead to the discovery of a correlation between the magnitude of the effective field gradient and the degree of metal-metal interaction.

The last obvious area of potential research is more esoteric in nature. The bonding models used in this study were very naive for several reasons. More sophisticated molecular orbital calculations directed toward the prediction of electron distributions in these studied compounds and other heavy transition metal compounds would serve as an independent check of some of the assumptions made here.

## ACKNOWLEDGEMENTS

The author greatly feels the contributions of many people to this thesis.

Dr. R. E. McCarley is to be envied for having the intellectual curiosity to encourage a student to pursue research not strictly within the major fields of his research interests. Too often students adapt their interests to those of the major professor; too rarely does a major professor modify his goals to a student's desires.

Thanks are also owed to Dr. R. G. Barnes and members of his Crystal Physics Group I, particularly Mr. D. R. Torgeson and Dr. W. C. Smith for their wit, wisdom, and patience. Without their experimental expertise this research would never have been completed.

Dr. C. B. Harris, Chemistry Department, University of California, Berkeley, had the "courage" to let an undergraduate student into his research group. Without that "boost" a graduate education would have been inaccessible to the author. One of his students, Dr. M. J. Buckley, is also thanked for his encouragement during and after that pivotal year.

Past and present members of Physical and Inorganic Group X too numerous to mention are thanked for their friendship during these four years. For the sake of their own sanities they are entitled to be thankful the author

is leaving.

To my parents, Mike and Rayna Edwards, can only go thanks for their unselfish aid. Their encouragement and support, not to mention other trivial details like their gift of life, made this thesis a reality.

The support and encouragement of my in-laws, Gene, Krys, and Tom Gardner, can also not go unrecognized; whipped cream cans and nipping dogs notwithstanding.

No words of thanks can adequately repay Ludy, my wife, for the trials and tribulations of being a graduate student's wife. She has made tangible contributions to the completion of this thesis, not only by typing preliminary and final drafts, but also by making every attempt possible to learn about my research activities. Trite or corny phrases do not adequately describe the intangible contributions she has made to my life since our meeting and the sacrifices and anxieties she has overcome during these four years. It must suffice to say that she truly is a woman among women. In the spirit of gratitude this thesis is dedicated to her.

## BIBLIOGRAPHY

- (1) H. Bayer, Z. Phys., 130, 227 (1951).
- (2) T. P. Das and E. L. Hahn, Solid State Phys., Suppl.,  
No. 1, (1958).
- (3) M. R. Jeffrey and R. L. Armstrong, Phys. Rev., 174,  
359 (1968).
- (4) R. P. Hamlen and W. S. Koski, J. Chem. Phys., 25,  
360 (1956).
- (5) A. H. Reddoch, Nuclear Quadrupole Resonance of Some  
Inorganic Compounds, USAEC, UCRL-8972 (1959).
- (6) A. Zalkin and D. E. Sands, Acta Crystallogr., 11,  
615 (1958).
- (7) I. Safin, B. Pavlov, and D. Shtern, Zavod Lab., 30,  
676 (1964).
- (8) R. Ikeda, D. Nakamura, and M. Kubo, J. Phys. Chem.,  
69, 2101 (1965).
- (9) T. E. Haas and E. P. Marram, J. Chem. Phys., 43,  
3985 (1965).
- (10) Yu. A. Buslaev, E. A. Kravchenko, S. M. Sinitsyna,  
and G. K. Semin, Izv. Akad. Nauk SSSR, Ser.  
Khim., 12, 2816 (1969).
- (11) H. G. Dehmelt, Phys. Rev., 92, 1240 (1953).
- (12) R. G. Barnes and S. L. Segel, J. Chem. Phys., 25,  
180 (1956).
- (13) R. G. Barnes, S. L. Segel, P. J. Bray, and P. A.  
Casabella, ibid., 26, 1345 (1957).
- (14) S. L. Segel and R. G. Barnes, ibid., 25, 578 (1956).
- (15) G. E. Peterson and P. M. Bridenbough, ibid., 51,  
238 (1969).
- (16) T. L. Brown, W. G. McDugle, Jr., and L. G. Kent,  
J. Amer. Chem. Soc., 92, 3645 (1970).

- (17) R. F. Fenske and D. D. Radtke, Inorg. Chem., 2, 479 (1968).
- (18) T. L. Brown and L. G. Kent, J. Phys. Chem., 74, 3572 (1970).
- (19) D. E. Sands and A. Zalkin, Acta Crystallogr., 12, 723 (1959).
- (20) R. L. Armstrong and G. L. Baker, Can. J. Phys., 48, 2411 (1970).
- (21) G. P. O'Leary and R. G. Wheeler, Phys. Rev. B, 1, 4409 (1970).
- (22) F. A. Cotton and C. B. Harris, Proc. Nat. Acad. Sci. U.S., 56, 12 (1966).
- (23) F. A. Cotton and C. B. Harris, Inorg. Chem., 6, 376 (1967).
- (24) J. E. Fergusson and E. E. Scaife, Inorg. Nucl. Chem. Lett., 7, 987 (1971).
- (25) D. E. Scaife, Aust. J. Chem., 24, 1315 (1971).
- (26) D. E. Scaife, ibid., 24, 1993 (1971).
- (27) T. B. Brill and G. G. Long, J. Phys. Chem., 75, 1898 (1971).
- (28) R. A. Mackay and R. F. Schneider, Inorg. Chem., 6, 549 (1967).
- (29) W. van Bronswyk and Sir Ronald Nyholm, J. Chem. Soc., A, 2084 (1968).
- (30) P. A. Edwards, R. E. McCarley, and D. R. Torgeson, Inorg. Chem., 11, 1185 (1972).
- (31) E. A. C. Lucken, "Nuclear Quadrupole Coupling Constants," Academic Press, New York, 1969.
- (32) R. H. Livingston and H. Zeldes, Table of Eigenvalues for Pure Quadrupole Spectra, Spin 5/2, USAEC, ORNL-1913 (1959).
- (33) M. H. Cohen, Phys. Rev., 96, 1278 (1954).

- (34) Y. Morino and M. Toyama, J. Chem. Phys., 35, 1289 (1961).
- (35) J. A. S. Smith and D. A. Tong, J. Chem. Soc., A, 173 (1971).
- (36) E. I. Fedin and G. K. Semin, Zh. Strukt. Khim., 1, 464 (1960).
- (37) G. K. Semin and E. I. Fedin, ibid., 1, 252 (1960).
- (38) C. H. Townes and B. P. Dailey, J. Chem. Phys., 17, 782 (1949).
- (39) B. P. Dailey, Faraday Soc. Discussions, 19, 255 (1955).
- (40) P. A. Casabella, P. J. Bray, and R. G. Barnes, J. Chem. Phys., 30, 1393 (1959).
- (41) M. Kaplansky and M. A. Whitehead, Can. J. Chem., 48, 697 (1971).
- (42) R. R. Smardzewski, Ph.D. Thesis, Iowa State University, Ames, Iowa, 1969.
- (43) M. A. Schaefer, Ph.D. Thesis, Iowa State University, Ames, Iowa, 1971.
- (44) G. E. Peterson and P. M. Bridenbough, Rev. Sci. Instrum., 37, 1081 (1966).
- (45) S. L. Segel and R. G. Barnes, Catalog of Nuclear Quadrupole Interactions and Resonance Frequencies in Solids. Part I. Elements and Inorganic Compounds, USAEC, IS-520 (revised) (1968).
- (46) P. M. Boorman, N. N. Greenwood, M. A. Hildon, and H. J. Whitfield, J. Chem. Soc., A, 2017 (1967).
- (47) R. G. Barnes and R. D. Engardt, J. Chem. Phys., 29, 248 (1958).
- (48) K. Mucker, G. S. Gordon, and Q. Johnson, Acta Crystallogr., 24B, 874 (1968).
- (49) V. S. Korol'kov and A. G. Makhanev, Optics and Spectroscopy, 12, 87 (1962).

- (50) C. H. Townes and A. L. Schawlow, "Microwave Spectroscopy," McGraw-Hill, New York, 1955.
- (51) B. J. Erisdon, D. H. Edwards, D. J. Machin, K. S. Murray, and R. A. Walton, J. Chem. Soc., A, 1825 (1967).

## APPENDIX

The first CPS program listed in this appendix, (F92,PAE), embodying the equations listed in Table II for the  $I = 9/2$  case, was used to calculate the four allowed resonance frequencies [RF(I)] for an  $I = 9/2$  spin nucleus. The two input parameters were the molecular coupling constant (CC) and the asymmetry parameter (ETA).

The second CPS program listed in this appendix, (BHR,PAE), embodying the appropriate equations listed in the Interpretation of Nuclear Quadrupole Resonance Data section of this thesis, was used to calculate bonding parameters for a bridging halogen atom. The three input parameters were the atomic coupling constant (CCA), the resonance frequency (RF), and the M-X<sub>b</sub>-M angle (AA). The calculated parameters were the molecular coupling constant (CCM); the asymmetry parameter (ETA); the square of the coefficient of the s atomic orbital in the hybrid bonding orbital wave functions (HYB); the electron populations of the hybrid, the s, the p<sub>x</sub>, and the p<sub>y</sub> orbitals (NA, NS, NPX, NPY respectively); and the total population of the bridging halogen atom (NT1 and NT2). (NT1 and NT2 must obviously be the same or an error has been made in the computations. They represent the same quantity only calculated in slightly different manners.) As it is now the program has several limitations. It is only useful for nuclei with  $I = 3/2$ , and for bridging angles (AA) in the range ca. 90 to 105°.

```
1.          /* FITTING OF I=9/2 RESONANCES */;
2.          /*P. EDWARDS 4-1136*/;
3.          DECLARE RF(4);
4.  JUNK:    GET LIST(ETA);
5.          GET LIST(CC);
6.          PUT LIST('      RF(1)      ');
7.          RF(1)=CC/24*(1+9.03333*ETA**2-45.6907*ETA**4);
8.          RF(2)=CC/12*(1-1.338095*ETA**2+11.7224*ETA**4);
9.          RF(3)=CC/8*(1-.18571*ETA**2-.12329*ETA**4);
10.         RF(4)=CC/6*(1-.08095*ETA**2-.004258*ETA**4);
11.         DO I=1 TO 4;
12.         PUT LIST(RF(I));
13.         END ;
14.         GO TO JUNK;
```

```

1.      /* FITTING OF BRIDGE HALOGEN RESONANCES */;
2.      /* P. EDWARDS 4-1136 */;
3.      GET LIST(CCA);
4.      GET LIST(RF);
5.      GET LIST(AA);
6.      BA=AA/2;
7.      HYB=-COSD(AA)/(1-COSD(AA));
8.      ETA=-3*COSD(AA);
9.      CCM=RF*2/(1+ETA**2/3)**.5;
10.     NA=2-CCM*(2*SIND(BA)**2)/CCA;
11.     NPX=NA;
12.     NS=2*(COSD(BA)/SIND(BA))**2+NA*(1-(COSD(BA)/SIND(BA))**2);
13.     NPY=2*(1-(COSD(BA)/SIND(BA))**2)+NA*(COSD(BA)/SIND(BA))**2;
14.     NT1=2+NS+NPX+NPY;
15.     NT2=4+2*NA;
16.     PUT LIST(' CCM ',CCM);
17.     PUT LIST(' ETA ',ETA);
18.     PUT LIST(' HYB ',HYB);
19.     PUT LIST(' NA ',NA);
20.     PUT LIST(' NS ',NS);
21.     PUT LIST(' NPX ',NPX);
22.     PUT LIST(' NPY ',NPY);
23.     PUT LIST(' NT1 ',NT1);
24.     PUT LIST(' NT2 ',NT2);

```